

## CHAPTER

## 122

## Functional Anatomy of the Neural Retina

Robert E. Marc

**Overview**

This chapter provides an outline of the organization of the mammalian retina, with a strong focus on primate vision and in the context of a nearly complete cellular catalog and extensive new understanding of the molecular diversity of signaling pathways. The mammalian neural retina, albeit simplified by evolutionary losses in cone-driven pathways, is proving to be more complex than anticipated, with over 60 classes of neurons, yielding at least 15 and perhaps 20 different ganglion cell 'filters' for the visual world. Elucidating the wiring of these filters for any retina remains a major challenge. Though several canonical signaling pathways have been mapped (including a novel scotopic path), we have not been able to reconstruct the likely networks of most of the filters. New discoveries regarding the molecular mechanisms of red and green cone visual pigment expression have profound implications for the development of color-selective circuits and color vision. A new ganglion cell class has intrinsic phototransduction mediated by a novel photopigment, melanopsin, and is selectively wired to at least three different functional pathways. Finally, the wiring of the retina is dynamic and manifests significant connectivity changes both under postnatal visual drive and retinal degenerations.

**INTRODUCTION**

The retina evolved to report spatiotemporal and chromatic patterns of photons imaged by the eye.<sup>1</sup> The plan of the human neurosensory retina is generically vertebrate in form and development, with key specializations. Photoreceptors form a discrete photon capture screen roughly similar in scale to a high-end color imaging chip (Fig. 122.1, panels 1–3).<sup>2</sup> Vertebrate retinas contain rods, cones, bipolar cells (BCs), horizontal cells (HCs), amacrine cells (ACs), association cells (AxCs), interplexiform cells (IPCs), and ganglion cells (GCs). Cones, BCs, and HCs connect to each other in the outer plexiform layer (OPL). BCs, ACs, AxCs, and GCs connect in the inner plexiform layer (IPL).

The basic vertical channel is the cone → BC → GC chain. Vertical channel signals are encoded by vesicular glutamate release (Fig. 122.2) and decoded by ionotropic or metabotropic glutamate receptors (iGluRs, mGluRs) expressed by target neurons.<sup>3–5</sup> Lateral channels mediate signal comparisons over time, space, or color via feedback and feedforward signaling. Lateral channels are numerous and include cone → HC → target cell transfers in the OPL and many BC → AC → target cell transfers in the IPL. AC signals are largely encoded by vesicular  $\gamma$ -aminobutyric acid (GABA) or glycine release (Fig. 122.2) and decoded by cognate receptors expressed on target cells.<sup>3,6</sup> HC signaling mechanisms remain in debate.<sup>7</sup>

Signaling in the IPL is also mediated by specialized AxCs (previously lumped with ACs) that signal over long distances with intraretinal axons.<sup>8</sup> The molecular determinants of signal amplification, signaling speed, signal integration, and memory systems associated with synaptic transfers will be reviewed in the context of cell-specific associations and canonical (main) pathways that encode and decode them.

Every species has a subtly different retina reflecting its distinctive evolutionary history. Features that are diagnostically vertebrate, mammalian, or primate will be noted when they highlight the special attributes of human vision. This chapter reviews the functional anatomy of primate and mammalian neural retinas in the context of discoveries that have revolutionized our understanding of the retinal cells and their associations (Box 122.1). The details of most of these discoveries are beyond the scope of this chapter but the era of purely descriptive neuroanatomy is past and new molecular, physiological, and connective contexts accompany descriptions of cell class. New technologies have revolutionized cell visualization and analysis, including cell specific reporter gene expression,<sup>9</sup> ballistic labeling,<sup>10</sup> and more. This knowledge is more than academic, as studies of animal models of human disease have revealed new dynamics in retinal neuroanatomy.<sup>11,12</sup> Neurodegenerative brain disorders and some slow photoreceptor degenerations similarly involve protein misfolding and proteasome stress.<sup>13</sup> In retina, as in brain, this stress induces anomalous neural rewiring. Ultimately, devising interventions that ameliorate vision impairment in macular degeneration, retinitis pigmentosa (RP), glaucoma, or vasculopathies will require in-depth understanding of the molecular nuances of contact specificity, signaling, cell form, and cell patterning in the retina.

**THE EVOLUTIONARY CONTEXT****INTRODUCTION**

Molecular biology has added new rigor to comparative biology. It is now clear that the mammalian retina reflects a major evolutionary reduction in neuronal diversity and a simpler structure than those of most other vertebrates. The genetics of that reduction is linked to an array of inherited eye defects. Every distinctive mammalian feature has been shaped by an evolutionary bottleneck that occurred over 200 million years (MY) ago in the late Triassic/early Jurassic as stem radiations of therapsid reptiles gave rise to early mammals (Fig. 122.3). This included the collapse of the ancestral mammalian axial skeleton, cranium, and visual system.

This sequence from early amniotes to mammals is the most fully documented of the major transitions in vertebrate

AU: 1.1, 1.2, 1.3, etc are changed to panel 1, panel 2, etc of Figure 122.1 OK? Please check.

## RETINA AND VITREOUS

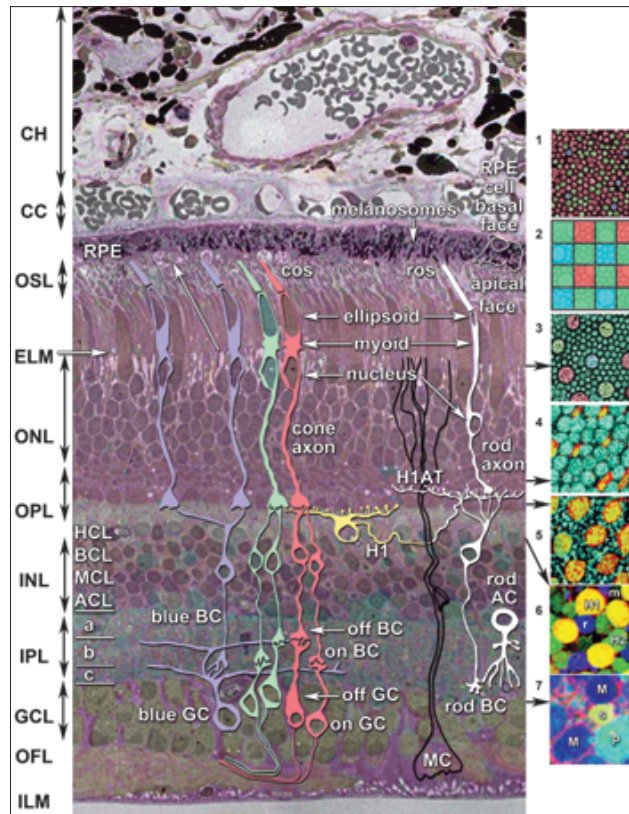


**FIGURE 122.1.** Cellular elements of the parafoveal primate retina (vertical plane, left panel; serial horizontal planes 1–7 at right). Schematics of cells are layered onto a computationally enhanced toluidine blue thin section of baboon retina (<http://prometheus.med.utah.edu/imagery.html>) taken at  $\sim 10^\circ$  eccentricity. The vascular supply for the sensory retina distal to the ELM is formed by the choroid (CH) and the choriocapillaris (CC), apposed to the basal surface of the RPE. Black cells in the CH are resident melanocytes; RPE cells contain dark melanosomes. The vascular supply for the neural retina proximal to the ELM is formed by capillary nets in the horizontal cell layer (HCL), amacrine cell layer (ACL) and distal GCL. Capillary lumens are marked with asterisks. Rod and cone outer segments (ros, cos) form a discrete layer (OSL) and abut the apical face of the RPE. Rod and cone inner segments extend to the OPL where they form their synaptic terminals: rod spherules and cone pedicles. Cones (tinted red, green, and blue) contact sets of ON and OFF BCs and the somas of HCs (e.g., H1 HCs), while rods (white) contact only rod BCs and the axon terminals of HCs (H1ATs). Cones distal to the ELM are gently tilted in the periphery proportional to their displacement from the visual axis. It is thought that they 'point' toward the nodal point of the eye at all eccentricities. The slight curvature is a defect of tissue processing. Cone BCs send their axons into the IPL to contact specific classes of cone GCs, while rod BCs contact rod-specific ACs. The INL in primate retina can be clearly divided into discrete HC, BC, MC and AC layers (HCL, BCL, MCL, ACL). The IPL is segmented into sublayers specific for the output synapses of OFF cone BCs (sublayer a), ON cone BCs (sublayer b), and rod BCs (sublayer c). The supporting glial MCs span the neural retina from the ELM to the inner limiting membrane (ILM), sealing the optic fiber layer (OFL) and GC layer (GCL) from the vitreous. Right: Seven horizontal plane views of the primate retina viewed as  $30\ \mu\text{m} \times 30\ \mu\text{m}$  patches. Panel 1: cone myoids in the foveola at the level ELM. Panel 2: cone and rod myoids at  $\sim 10^\circ$  in the periphery with a Bayer-filter overlay (see text). Panel 3: Panel 2: cone and rod myoids at  $\sim 10^\circ$  in the periphery. Panel 4: Rod spherules (cyan) interspersed with cone axons (red-yellow). Panel 5: Cone pedicles (red-yellow) surround by processes of rod BC and HC axon processes. Panel 6: HCL. H1 HCs (yellow); H2 HCs (bright green); rod BCs (blue, r); MCs (black, m). Panel 7: GCL. Midget GCs (Blue, M), parasol GCs (Cyan, P), starburst ACs (s, yellow). All images are at the same scale and each square is  $30\ \mu\text{m}$  wide. © REM 2006.

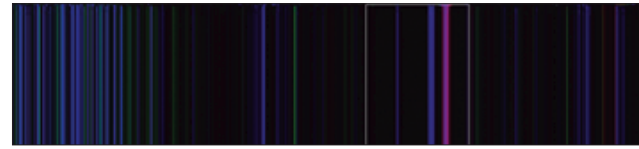


**FIGURE 122.2.** Visualization of GABA (red), glycine (green), and glutamate (blue) signals in the primate retina. Glutamate signals are enriched in rods, cones, BCs, and GCs. Glycine signals are preferentially enriched in a subset of ACs with sparse terminals. GABA signals are expressed by a large subset of ACs with widely distributed terminals. Mixed GABA–glutamate magenta signals are expressed by a subset of BCs in some primates. MCs express little or no glutamate, GABA or glycine and appear black. Each of these signatures can be resolved in the IPL as synaptic terminals or processes from each of these cell classes (inset). The image is  $0.9\ \text{mm}$  wide. © REM 2005.

### BOX 122.1 Key advances in retinal anatomy in the past decade

- The assembly of a nearly complete cellular catalog
- The assembly of a primitive catalog of transcriptional regulators of cell phenotype
- New connectivity implications of primate VP gene evolution
- Neuronal phototransduction in melanopsin-expressing GCs
- Neural plasticity in the developing and mature retina
- Circuitry remodeling in retinal disease
- Extensive molecular understanding of the diversity, function and cellular dispositions of
  - glutamate-gated AMPA, KA, NMDA, and mGluR receptors
  - GABA-activated and glycine-activated receptors
  - glutamate, GABA, glycine, and anion transporters
  - calcium channels, CNG channels, other ion channels
  - connexins
- Resources of particular value
  - Oyster. The Human Eye. 1999 Raven Press. A wonderful, readable and comprehensive book on functional anatomy of the human eye
  - The Visual Neurosciences Vols 1 and 2 (Chalupa and Werner, eds), MIT Press. 2004 A detailed treatment of visual system signaling structures and mechanisms
  - Webvision: <http://webvision.med.utah.edu>. A comprehensive and dynamic resource.

AU: Please supply 'Key Features'

evolution. The entire skeleton was modified, as was the soft anatomy, behavior, and physiology down to the level of cellular metabolism. Many of these changes are demonstrated, either directly or indirectly, through the fossil record.<sup>14</sup>

The adoption of a nocturnal, fossorial, and insectivorous niches by early mammals triggered the loss of over half the retinal neuron phenotypes still manifested by extant non-mammals (Tables 122.1 and 122.2). The dominant visual stream was switched from the color-rich nonmammalian collothalamoc stream (retina  $\rightarrow$  tectum  $\rightarrow$  N. rotundus  $\rightarrow$  ectostriatum) to the largely achromatic lemnothalamoc stream (retina  $\rightarrow$  lateral geniculate nucleus (LGN)  $\rightarrow$  striate cortex). Further, the widespread epithalamic (pineal and parapineal parietal) pathways disappeared in mammals as functional photo-sensitive systems. The following sections summarize the major evolutionary revisions of mammalian and primate retinas.

AU: Please check the sentence "Panel 3: Panel 2: cone and rod myoids at  $\sim 10^\circ$  in the periphery." OK?

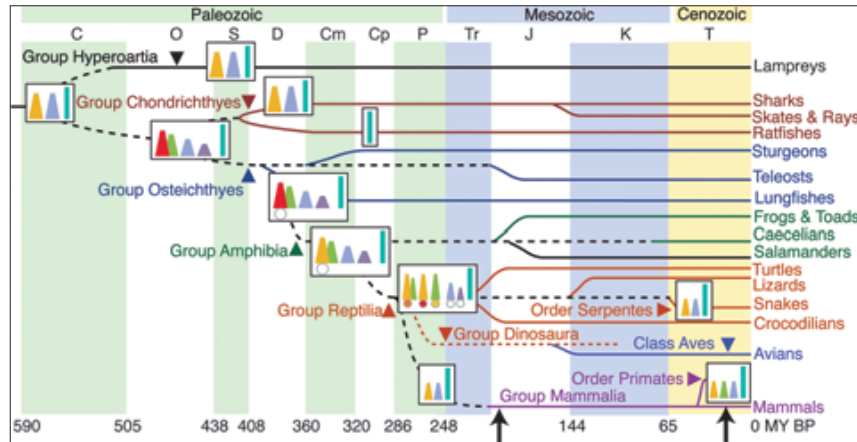


**FIGURE 122.3.** Spectral mixtures of rods and cones mapped on the evolution of the major vertebrate taxa. Solid lines indicate a continuous fossil record; dashes indicate gaps. Cone LWS, cone SWS1 and rod RH1 VPs (see text) evolved early and were likely expressed by Cambrian ancestors of the lampreys (Group Hyperoartia, yellow cone, blue cone, and green rod icons). These pigments were extensively diversified during the evolution of the Osteichthyes to include LWS cones (red icons), RH2 cones (green icons), SWS1 cones (blue icons), and SWS2 UV cones (violet icons), as well as rods. This diversity persists in modern descendent groups (Amphibia, Reptilia, Aves). With the evolution of mammals at 200–240 MY BP (million years before present, arrow), the RH2 and SWS2 systems were lost. Roughly 20 MY BP (arrow), trichromatic primates evolved a new green pigment from the LWS system. C, Cambrian; O, Ordovician; S, Silurian; D, Devonian; Cm, Carboniferous Mississippian; Cp, Carboniferous Pennsylvanian; P, Permian; Tr, Triassic; J, Jurassic; K, Cretaceous; T, Tertiary.  
© REM 2004.

**TABLE 122.1.** Retinal Attributes of the 7 Vertebrate Classes and Primates

	CI Hyperoartia	CI Chondrichthyes	CI Osteichthyes	CI Amphibia	CI Reptilia	CI Aves	CI Mammalia	Order Primates
Divergence MY	< 500	450	417	500	500	500	200	200
Cone classes	3	0–2 ?	3–7	4	3–7	3–7	0–2	2–3
Rod classes	1	1	1	1–2	1–2	1	1	1
Rod pathway	Direct	Direct	Direct	Direct	Direct	Direct	Indirect	Indirect
Neuronal classes	?	?	>120	>100	>100	>100	50–60	50–60
Distinct ACs, or foveas	0	0	0–1	0–1	0–1	0–2	0–1	1
Intraretinal vessels	—	—	—	—	—	—	+	+
Pineal / parietal organs	1	1	1	2	2	1	0	0

Divergence is the time in millions of years (MY) before present that the taxon is clearly identified in the fossil record. Cone classes are defined by combined opsin expression and structural phenotype. Neuronal classes are identified by morphology.

**TABLE 122.2.** Neuronal Diversity in Selected Mammals Compared with a Teleost Fish

	Goldfish	Mouse	Cat	Rabbit	Macaque	Human
Cone classes	7	2	2	2	3	3
Cone chromatotypes	7	2	2	2	2	2
Cone visual pigments	4	2	2	2	3	3
Horizontal cells	4	1	2	2	3	3
Bipolar cells	~20	~10	~12	~12	~12	~12
Amacrine cells	>70	?	?	~30	?	?
Ganglion cells	>20	?	~20	>15	?	?

AU: What does '?' stand for in all tables? Please check.



## RETINA AND VITREOUS

### THE REEVOLVED MAMMALIAN ROD CIRCUIT

Mammalian rod circuits represent a complex revision of ancestral scotopic vision. The primary mammalian rod pathways are now well understood as the following stream<sup>4,15-18</sup>:

rods → rod BC → rod (AII) AC → cone BCs → cone GCs

Remarkably, this pathway loops back into cone pathways after traversing the entire retina. It has no known antecedent in any other vertebrate group. In most nonmammals, rods and cones share BCs and scotopic paths to the brain are direct: rods → BCs → GCs → CNS.<sup>19</sup> The mammalian rod AC must have developed from an extant but still unknown nonmammalian sister cell. The molecular genetics of rod pathway development,<sup>20-22</sup> especially comparative patterns of transcriptional regulation and growth factor signaling across vertebrates, is likely the key to discovering how the rod circuit lost direct access to GCs. That knowledge may be central in learning how to repair wiring anomalies in retinal degenerations.

### REDUCTION OF THE IMAGE-FORMING CONE COHORT TO TWO TYPES: LWS AND SWS1

Old-world primate retinas express three cone classes: red-sensitive, green-sensitive, and blue-sensitive or R, G, B cones (Box 122.2). The massive loss of cones and reduction in cone diversity was the prelude to creating a predominantly nocturnal retina. Some mechanism must have repressed cone progenitor proliferation and enhanced rod progenitor expansion. Again, this history is not merely of academic interest, since defects in these genes are associated with eye degenerations. In most nonmammals (>95% of all vertebrate species), color-coding pathways are constructed from 3 to 6 structurally distinct cone types predominantly expressing one of 3–4 cone visual pigment (VP) genes,<sup>23</sup> as well as many distinctive neurons that selectively contact those classes. Each cone is a member of a chromatotype: a phenotype complex that includes genes for cone shape, patterning, and connectivity in addition to VP expression. It would not be surprising if red and green cone phenotypes in nonmammals differed in expressions of tens-

to-hundreds of genes. In contrast, primate red and green cone phenotypes may differ in only one gene: the VP.

Mammals, including primates, express cone VPs derived from two primordial gene groups (long-wave (LWS) and short-wave (SWS1) systems) yielding retinas with two cone chromatotypes: green-yellow and violet-blue absorbing. SWS1 cones differ from LWS cones in timing of developmental emergence, spatial patterning, subtleties of shape (in primates) and connectivity.<sup>24-26</sup> Within the past 30–40 MY, a gene duplication event resulted in the formation of a tandem head-to-tail array of red ( $\lambda_{\max} \sim 560$  nm) and green ( $\lambda_{\max} \sim 530$  nm) pigment genes on the primate X chromosome.<sup>27</sup> Historically, primate red and green cones have been viewed as the initiators of separate color channels, with separate connectivities leading to hard-wired color-opponent neural assemblies at the GC level. This deterministic model is now in doubt; a stochastic process likely controls whether a cone stably expresses green or red pigment.<sup>28</sup> Thus it is difficult to see how pathway-specific genes could be specifically coupled to a green or red phenotype. All mammals may express only two image-forming cone chromatotypes and this would reduce the required diversity of retinal neurons and the number of neuron types.

The full set of cone chromatotypes may not yet be in hand. Recently, a sparse, orderly population of novel cones has been described in mouse retina that exclusively expresses a vesicular glutamate transporter type vGlut2.<sup>29</sup> Further, a small set of human cones has been shown to express melanopsin, a novel photosensitive pigment.<sup>30</sup>

### REDUCTION OF NEURONAL DIVERSITY

Over half of the retinal neuron classes expressed by nonmammals have been lost in the mammalian retina (Table 122.1), including many cone-driven HC, BC, AC, and GCs. In addition to expressing more than three cone chromatotypes, some nonmammals possess as many as four HC, >20 BC and >70 AC classes (Table 122.2). Further, there are likely at least four classes of IPCs in teleost fishes<sup>31</sup> and none of their homologs have been identified in mammals. Most teleost IPCs evolved fairly recently; i.e., they are apomorphic. However, glycinergic IPCs are expressed by pre- and post-osteichthyan vertebrates and are thus ancient.<sup>31</sup> But they are absent in mammals. While tools to precisely classify all neuronal classes are still emerging, it is clear that the mammalian retina represents a reduced set of antecedent neuron classes that have persisted in other taxa.

### APPARENT LOSS OF NEURAL RENEWAL MECHANISMS

One of the more remarkable features of many nonmammalian retinas is the persistence of neuronal progenitor cells in the eye throughout life, near the retina and perhaps in the retina. In fishes, rod progenitor cells are known to be able to migrate far from the progenitor-rich ciliary marginal zone, a torus some 10–20 cells thick interposed between the termination of the retina and the ciliary epithelium.<sup>32</sup> The amphibian marginal zone is similar and some urodele amphibians can regenerate an entire retina at any point in life. There is also evidence that new photoreceptors and retinal neurons can replace damaged patches in mature fish retinas and that glial Müller cells (MCs) can proliferate and may even become neuroprogenitor cells. The mammalian retina lacks these robust processes, as far as is known though small clusters of potential neuroprogenitor cells have been found at the mammalian retinal margin.<sup>33</sup>

#### BOX 122.2 Issues in naming cones

- Two schemes have been used: RGB (red, green, blue) and LMS (long-, mid-, and short-wave)
- The LMS system denotes a cone's *relative* spectral peak to avoid confusion between perceptual names (red, green, blue) and VP absorption peaks (yellow-green, green, violet)
- The LMS system is adequate for mammals, but is awkward for nonmammalian species that express four cone VPs and up to seven chromatotypes
- A rich tradition of primate CNS physiology exploits the RGB terminology
- The LMS system can be confused with VP gene groups: primate L and M cones are group LWS cones; fish L and M cones are group LWS and Rh2 cones, respectively
- Perceptual channels initiated by RGB cones do match color names well
- Increment threshold spectral sensitivities of trichromatic primates show three peaks: 610 nm (orange-red), 535 nm (green), and 430 nm (blue), each primarily driven by R, G, or B cones

## NEW RETINAL ENERGETICS AND VASCULARIZATION

The success of the mammals was largely due to the emergence of a lightweight vascularized skeleton, a more space-efficient cortical expansion, endothermy, and improved respiratory and vascular systems.<sup>14</sup> The mammalian retina is the only truly vascularized retina.<sup>1</sup> However, this bias toward high mitochondrial energy supply engages several risks. The first is poor tolerance of low oxygen tensions. Aquatic species, even those that demand high oxygen levels (e.g., salmonids), are also remarkably resistant to both hypoxia (a common event in fresh water environments) and hyperoxia.<sup>34</sup> The neural retinas of turtles and tortoises are thick, contain perhaps triple the number of neuronal classes as mammals, have complex chromatic processing and high-acuity fovea-like specializations, but are robust in hypoxic settings. Second, the mammalian dependence on high-speed blood gas and metabolite transport via fine capillary networks in the OPL and IPL entails significant light scattering and demands that MCs play an active role in retinal homeostasis by investing the endothelial layer in the same manner as protoplasmic astrocytes in brain.<sup>1</sup> Finally, the unique vascularization of the mammalian retina also exposes it to the danger of renewed angiogenesis.

## THE FUNDAMENTALS OF RETINAL STRUCTURE

### THE LAYOUT OF THE NEURAL RETINA

The retina is designed to do two things; sample the torrent of photons in the retinal image plane and edit the neural signals produced by photoreceptors into several sets of filtered neural images.<sup>1</sup> This requires a large number of sensory cells, neurons, glia, and supporting epithelia and vasculature. Like most brain nuclei, the retina is a lattice of neurons framed by glia and sealed from its supporting vasculature (Fig. 122.1). At the outer (distal, sclerad) retinal margin (Box 122.3), the retinal pigmented epithelium (RPE) forms coupled, high-resistance basolateral barrier between the endothelia of the choroicapillaris and the outer segments of the photoreceptors next to the RPE apical face. At the inner (proximal, vitread) retinal margin, the end feet of MCs and sparse astrocytes in the optic fiber layer form an intermediate junction seal between neural retina and vitreous. Between these two seals, vascularized mammalian retinas contain four dense capillary nets; two bordering the inner nuclear layer (INL) and two bordering the ganglion cell layer (GCL).<sup>1</sup> The retina is functionally partitioned into outer *sensory* and inner *neural* layers. The sensory layer is composed of rod and cone photoreceptors, surrounded by distal MC processes. Similar to other high-gain sensory systems, the sensory layer is separated by the external limiting membrane (ELM) into ionically distinct distal and proximal extracellular compartments. The ELM is a precise border of macromolecule-impermeant

intermediate-junctions between MCs and photoreceptors (Fig. 122.1). The ELM and the basolateral tight junctions of the RPE delimit the subretinal space; a dynamic regime transited by high fluxes of water, oxygen, bicarbonate, protons, inorganic ions, sugars, amino acids, osmolytes, and retinoids. The part of the MC proximal to the ELM is responsible for regulating a similar array of moieties in the neural retina, in addition to critical recycling of carbon skeletons derived from synaptic overflow of glutamate and GABA.<sup>3</sup> MCs ensheath the entire neural retina, comprising ~30% of the INL in the primate central retina and up to 50% in the far periphery.<sup>35</sup> This vertical view masks the elegant spatial tiling of the retina. At the level of the ELM in the foveola, an array of ~160 000/mm<sup>2</sup> cone myoids sample visual space with apertures of <2  $\mu$ m each (Fig. 122.1, panel 1). In the near periphery, where cone density drops to ~9000/mm<sup>2</sup> (Fig. 122.1, panels 1 and 3) large cone apertures are evenly distributed in a matrix of rods that have nearly the same density as foveolar cones, i.e., 150 000/mm<sup>2</sup>. The same field is also shown with a scale overlay of a Bayer-style filter<sup>2</sup> for color-imaging chips, with a conventional 7.5  $\mu$ m pixel size (Fig. 122.1, panel 2). This fine screen of rod and cone apertures is remapped into separate arrays of rod and cone synaptic terminals (Fig. 122.1, panels 4 and 5). Because rod spherules are so large (>2  $\mu$ m diameter), they cannot be packed into a single plane and, at this eccentricity, are stacked four deep, just distal to the layer. Some extracellular matrix mechanism may control this precise lamination. Foveolar cones have long axons (fibers of Henle) that spray out like an aster from the central foveola and array their pedicles into a ring packed edge-to-edge in a single tile layer. As the cone density drops, the tile spacing increases and in the periphery the cone pedicle mosaic roughly maps onto the myoid mosaic. Just beneath the pedicles, diverse classes of HCs and BCs form rough patterns to cover image space (Fig. 122.1, panel 6), ultimately converging on a complex tiling of GCs (Fig. 122.1, panel 7).

### BASIC NEURONAL PHENOTYPES

There are two major retinal neuron phenotypes; sensory neurons and multipolar neurons. The sensory neuron phenotype includes rods, cones, and BCs (Fig. 122.1), all of which display essential attributes of a polarized epithelium.<sup>36</sup> Cells of the sensory phenotype possess the following distinctive features:

- Ciliary apical and secretory basal specializations characteristic of polarized epithelium
- Apical poles specialized as photoreceptor outer segments or BC dendrites
- G-protein coupled receptor-mediated transduction (e.g., photoreceptors and ON BCs)
- Basal poles specialized as a single axon terminating in a secretory synaptic ending
- Synaptic release driven by high-capacity ribbon-assisted vesicle fusion
- A glutamatergic phenotype

The multipolar neuron phenotype includes ACs, AxCs, and GCs and these display classic projection or local circuit neuron features:

- Ovoid somas with weak apical-basal polarization
- One to many primary dendrites arising from one hemisphere of the cell
- One or more classical axons in many cell types
- Both axons and dendrites can form many synaptic sites
- Synaptic release driven by low-capacity conventional vesicle fusion
- ACs tend to be GABAergic or glycinergic
- GCs are predominantly glutamatergic

#### BOX 122.3 Glossary of orientations

Term	Reference Object	Use
Sclerad → Vitread	Layers of the eye, outside → inside	Global location in the eye
Outer → Inner	Layers of the eye, outside → inside	Fine tissue layering
Distal → Proximal	Distance from the CNS, far → near	Position along a neural chain
Vertical → Horizontal	Image plane, normal → parallel	Histologic plane of view

AU: Please provide expansion of ON?

## RETINA AND VITREOUS

HCs have no clear homology to either bipolar or multipolar cells and been provisionally designated their own phenotype. Though HCs appear multipolar, express iGuRs, and respond directly to photoreceptors, they have a number of anomalous features:

- Few or no defined presynaptic sites
- Unresolved synaptic signaling mechanisms
- Nonspiking axons that appear longer than their cable space constant
- Direct contact with capillaries
- Unresolved neurotransmitter phenotypes
- Intermediate filament expression characteristic of glia

### SIGNALING MECHANISMS

Neurons encode their voltage signals as changing rates of neurotransmitter release and decode incoming neurotransmitter signals via transmembrane receptors. Neurotransmitter systems of the vertebrate retina have been extensively reviewed<sup>3,6,37</sup> and will be summarized only briefly. Many types of vertebrate sensory neurons use ribbon synapses<sup>37</sup> for high rates of tonic release, while multipolar neurons use conventional synapses.<sup>37</sup> Photoreceptors and BCs are glutamatergic neurons and use ribbon synapses for release. Each photoreceptor uses a single specialized presynaptic terminal containing on the thousands of vesicles and ribbon-associated vesicle fusion sites that mobilize a smaller releasable pool of vesicles.<sup>18</sup> Rods contain one or two ribbon sites<sup>38</sup> and large primate cones contain ~20–50. BCs use branched axon terminals that contain similarly large numbers of ribbon synapses. The ribbon is a mechanism for collecting vesicles at high density near the membrane fusion active zone and such synapses are capable of sustained fusion at 500–2000 vesicles/s.<sup>39</sup> In general, ACs are either GABAergic or glycinergic neurons and use conventional synapses for release. Each AC cell contains hundreds of small presynaptic assemblies ranging in size from 10 to 1000 vesicles and specialized for low release rates (20–100 vesicles/s).<sup>40</sup> GCs are generally glutamatergic, project to central targets and use conventional synapses.<sup>1,3</sup> The diversity of coding and signaling mechanisms is summarized in Boxes 122.4 and 122.5. We are still untangling the molecular mechanisms of these processes. For example, four different glutamate subunit genes (*GluR1–4*) produce many post-translationally modified proteins that can apparently associate in any stoichiometry, generating AMPA receptors with different glutamate affinities, conductances, kinetics, and co-protein associations.<sup>3</sup> Box 122.5 summarizes the ionic mechanisms mediated by the major signaling pathways in the retina.

### THE NEURON SET AND ITS CONNECTIVITY

Box 122.6 summarizes the neuronal classes in the mammalian retina. Signals from rods and cones diverge to at least 10 distinct BC classes (4) and thence into ~15 GC<sup>42,43</sup> and ~30 AC classes.<sup>44</sup> Ultimately, photoreceptor signals drive at least 15 distinct synaptic chains of neurons representing different filtered versions of the visual world. Each of these chains represents a distinct class of sampling unit with biases toward various stimulus qualities.

Each retinal neuron collects photoreceptor signals from specific synaptic chains. GCs collect direct signals from cone → BC → GC vertical channels and indirect signals that pass through lateral channels containing HC or AC elements (Fig. 122.4). This collection of vertical and lateral signals is combined by the target neuron to form its receptive field: a response waveform ↔ stimulus map. In the simplest receptive fields, a patch of light generates a single response polarity, such

#### BOX 122.4 Encoding molecules and decoding molecules

Many different small transmitter molecules are used to *encode* retinal signals:

- Glutamate is used by photoreceptors and BCs for fast vertical channel signaling
- GABA is used by AC subsets for fast lateral inhibition, usually *within* IPL strata
- Glycine is used by AC subsets for fast lateral inhibition, usually *across* IPL strata
- Acetylcholine (ACh) is used by starburst ACs for fast lateral excitation *within* IPL strata
- Dopamine (DA) is used by large AxCs for slow modulation events
- Nitric oxide is used by many cells and certain AxCs for slow modulation events
- Peptides are produced by both ACs and AxCs for modulatory signaling
- Melatonin is produced by photoreceptors in a diurnal pattern

Different macromolecules are used to *decode* retinal signals and most cells express more than one:

- All cells express ionotropic (iGluR) and/or metabotropic (mGluR) glutamate receptors
- mGluR6 receptors are fast, high-gain, and sign-inverting group C mGluRs (ON BCs)
- AMPA receptors are fast, medium-gain, and sign-conserving iGluRs (OFF BCs, HCs, ACs, GCs)
- KA receptors fast, high-gain, and sign-conserving iGluRs (OFF BCs)
- NMDA receptors are slow, low-gain, and sign-conserving iGluRs (some ACs, most GCs)
- GABA<sub>A</sub> ionotropic receptors are fast, low-gain, and sign-inverting (BCs, ACs, GCs)
- GABA<sub>B</sub> metabotropic receptors are slow, high-gain, and sign-inverting (mostly BCs)
- GABA<sub>C</sub> ionotropic receptors are slow, high-gain, and usually sign-inverting (mostly BCs)
- Gly ionotropic receptors are fast, low-gain, and sign-inverting (BCs, ACs, GCs)
- nACh receptors are fast, high-gain, and sign-conserving (GC subsets)
- mACh receptors are slow, high-gain, and usually sign-inverting (AC subsets)
- DA1 receptors are very slow, low-gain, and usually increase cAMP levels in many cells
- DA2 receptors are very slow, high-gain, and usually decrease cAMP levels in many cells
- Nitric oxide activates soluble guanylyl cyclase and raises cGMP levels in many cells

as cone responses to small spots. Most BCs and GCs possess concentric center-surround receptive fields,<sup>45</sup> where vertical channels drive a center response and lateral channels generate annular surrounds of opposite polarity (Fig. 122.5). More complex fields encode time-dependent events.

### PHOTORECEPTORS – STAGE 1 OF THE VERTICAL CHANNEL

The primate retina possesses three image-forming photoreceptor chromatophores.

- Rods express the RH1 opsin group VP 499, have a unique rod structural phenotype, and selectively contact rod BCs and HC axon terminals.

**BOX 122.5 Five major signaling mechanisms**

- **Metabotropic photoreceptor > ON BC signaling**  
Glutamate released by photoreceptors binds to mGluR6 and initiates a G protein signal cascade thought to lead to the closure of nonselective cation channels permeant to Na<sup>+</sup>, K<sup>+</sup>, Ca<sup>2+</sup>, and Mg<sup>2+</sup>. As photoreceptors hyperpolarize, intrasynaptic glutamate levels drop and unbound mGluR6 becomes permissive of cation channel opening, increasing Δg and depolarizing ON BCs through an inward cation current.
- **Ionotropic photoreceptor > HC and OFF BC signaling, BCs > AC and GC signaling**  
Glutamate released by photoreceptors or BCs binds to iGluRs and initiates the opening of nonselective cation channels, increasing Δg and depolarizing target cells through inward cation currents. As photoreceptors or BCs hyperpolarize, intrasynaptic glutamate levels drop, unbound iGluRs gate cation channel closure and hyperpolarize target neurons.
- **Ionotropic AC > i BC, AC, and GC signaling**  
GABA or glycine release from ACs binds to ionotropic GABA or glycine receptors and initiates the opening of a nonselective anion channel (Cl<sup>-</sup> is the prime permeant), increasing Δg and hyperpolarizing target cells through inward anion currents. When these currents are large, they constitute hyperpolarizing inhibition. Unlike cation conductances, anion conductances often operate near the chloride equilibrium potential and polarization changes may be small. Even so, Δg may be large, constituting shunting inhibition.
- **Metabotropic AC > BC and GC signaling**  
GABA release from ACs binds to metabotropic GABA receptors and initiates a G protein signal cascade thought to lead to (1) a desensitization of the voltage sensitivity of BC synaptic Ca<sup>2+</sup> channels, depressing glutamate release or (2) opening of voltage-gate K<sup>+</sup> channels, increasing Δg and hyperpolarizing target cells through outward K<sup>+</sup> currents.
- **Gap junction signaling**  
Gap junctions composed of connexin rafts permit direct sign-conserving current flow between pairs of identical (homocellular coupling) or different (heterocellular coupling) neuron classes. Slow signals (dopamine, NO) can modulate connexin conductance.

- Blue cones express the SWS1 opsin group VP 420, have a subtle but unique blue cone morphology, contact cone BCs and HCs, with a strong preference for a blue ON BC.
- Red and green cones express VP 530 or VP 560 from the LWS opsin group, are structurally indistinguishable from each other, contact cone BCs and HCs, but avoid the blue ON BC.

Rod and cone photoreceptors are complex, polarized sensory neurons (Fig. 122.6) whose structures and biologies are detailed in the following chapter. Peripheral primate rods and cones are cylindrical cells ~70–80 μm long, each possessing a sensory outer segment ~10–30 μm long (species-dependent) and a larger, neuron-like inner segment. Rods and cones exhibit significant functional similarity to fiber optics and 'guide' captured photons. Primate rod outer segments and the optically active inner segment portion have a diameter of ~1.5 μm. Large diurnal or crepuscular mammals such as primates have large cones with optically active inner segment diameters of ~5–7 μm, yielding a large photon-capture cross section. In contrast, both rods and cones of mouse are small and ~1–2 μm in

**BOX 122.6 Retinal neuron phenotypes**

1. The Sensory Neuron Phenotype (bipolar shape, ribbon-based vesicle fusion)
  - 1.1. Photoreceptors (VP family = class)
    - 1.1.1. Red/Green Cones (Stochastic LWS VP530 or LWS VP560, 1 class)
    - 1.1.2. Blue Cones (SWS1 VP 410, 1 class)
    - 1.1.3. Rods (RH1 VP499, 1 class)
  - 1.2. Bipolar Cells
    - 1.2.1. ON Bipolar Cells (mGluR6 expression)
      - 1.2.1.1. Rod ON Bipolar Cells (1 class)
      - 1.2.1.2. Blue Cone ON Bipolar Cells (1 class)
      - 1.2.1.3. RGB Cone ON Bipolar Cells
        - 1.2.1.3.1. Midget ON Bipolar Cells (1 class)
        - 1.2.1.3.2. Diffuse ON Bipolar Cells (~3 or more classes)
    - 1.2.2. OFF Bipolar Cells (iGluR expression)
      - 1.2.2.1. RG or RGB Cone OFF Bipolar Cells
      - 1.2.2.2. Midget OFF Bipolar Cells (1 class)
      - 1.2.2.3. Diffuse OFF Bipolar Cells (~3 or more classes)
2. The Multipolar Neuron Phenotype
  - 2.1. Projection Cells (axon-bearing, spiking)
    - 2.1.1. Ganglion Cells (>15 classes)
    - 2.1.2. Association Cells (>6 classes)
  - 2.2. Local Circuit Neurons
    - 2.2.1. Lateral Amacrine Cells (mostly GABAergic, 20–25 classes)
    - 2.2.2. Vertical Amacrine Cells (mostly Glycinergic, 5–10 classes)
3. The Horizontal Cell Phenotype (2–3 classes)

optical diameter. The outer segment is an expansion of the membrane enclosing single nonmotile cilium to form hundreds to thousands of rod disks or cone lamellae specialized for photon capture and signal transduction. The cilium provides microtubule-based bidirectional transport of cytosolic proteins. The dominant membrane proteins, opsins, are delivered to nascent discs and lamellae via a targeted vesicle fusion pathway surrounding the cilium. Just proximal to the cilium is the ellipsoid region of the photoreceptor; an array of longitudinally oriented mitochondria providing high rates of ATP production for visual transduction and Na<sup>+</sup>/K<sup>+</sup> ATPase in the inner segment. Primate cone ellipsoids are ~6–8 μm in diameter and ~12 μm long (a gross volume of ~340 fL), precisely positioned in a single band centered ~8 μm distal to the ELM in peripheral retina. Primate rod ellipsoids are 20-fold smaller in volume. In contrast, both mouse rod and cone ellipsoids are small and similar to primate rods.<sup>46</sup> This is an important neuro-anatomical distinction. First, the energetics of mouse cones are likely specialized for use in crepuscular contexts, rather than the high bleach rates of the noon-time savannah. Second, as the mouse model has become a key tool for understanding human retinal disease, these energetic differences associated with cone size may be relevant to interpreting disease progression. Mouse cones appear quite susceptible to indirect or bystander killing in some retinal degenerations,<sup>11,47</sup> while human cones seem much more resistant.

The component of most relevance to this chapter is the photoreceptor synaptic terminal (Fig. 122.7). Mammalian rod synaptic terminals are termed spherules and are spheroids of ~2 μm in diameter. Each rod axon terminates in a single spherule containing thousands of synaptic vesicles, one or two synaptic ribbons that serve as vesicle tethering stations next to



## RETINA AND VITREOUS

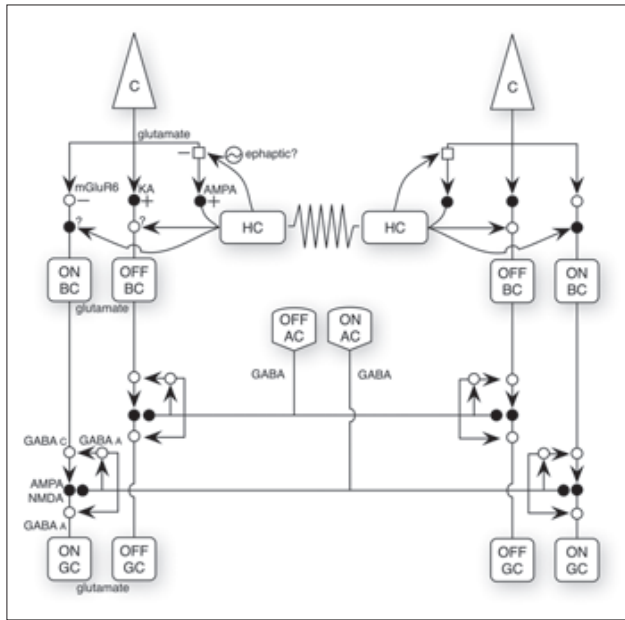


**FIGURE 122.4.** The basic cone-driven elements of the retina. Vertical channels are formed by cone → BC → GC chains. Cones (C) are presynaptic (arrows) to ON BCs via sign-inverting (○) mGluR6 receptors, OFF BCs via sign-conserving (●) KA receptors, and HCs via sign-conserving AMPA receptors. ON BCs and OFF BCs drive matched ON ACs/GCs and OFF ACs/GCs via sign-conserving AMPA and NMDA receptors. Surround channels are formed by HCs in the OPL and ACs in the IPL. HCs are coupled into homocellular networks by gap junctions (resistor symbol) and engage in feedback onto cones and feedforward onto BCs. The mechanisms of these feedback schemes are not well understood (see text), but it has been argued that HC → cone signaling could be ephaptic (□), rather than transmitter-mediated. GABAergic ACs dominate feedback and feedforward in the IPL via sign-inverting synapses, usually of complex receptor composition. AC → BC signaling is dominated by GABAC receptors, while AC → GC and AC → AC signaling are dominated by GABAA receptors.

© REM 2006.

the vesicle fusion sites of the spherule presynaptic membrane,<sup>40</sup> many multivesicular bodies thought to represent synaptic vesicle recycling pathways, and apparently one mitochondrion. The glutamate signal from each rod spherule's synaptic vesicle release is 'sampled' by two to four fine rod BC dendritic processes and one to four lobular HC axon terminal processes.<sup>40</sup>

Mammalian cone synaptic terminals are termed pedicles, and they have the shape of an architectural pediment, with a 2 μm axon at the peak widening to a base width of >5 μm in primates. Each cone axon terminates in a single pedicle containing many thousands of synaptic vesicles, ~50 or more synaptic ribbons,<sup>48</sup> multivesicular bodies, and a larger mitochondrial volume than rods. The glutamate signal from each ribbon site is sampled by several cone BC and HC dendrites, and each cone pedicle in this is sampled by hundreds of dendrites from 8 to 12 different cell classes.

There is weak electrical coupling mediated by small gap junctions between the pedicles of neighboring cones, between spherules of neighboring rods, and between cone pedicles and rod spherules, mediated by connexin36.<sup>49–52</sup> Rod-cone coupling (Fig. 122.8) allows rod signals to enter the cone pathway at high scotopic levels. Coupling also occurs between pairs of cones. Evidence from the dichromatic ground squirrel show that LWS green and SWS1 blue cones do not form G–B coupled pairs,

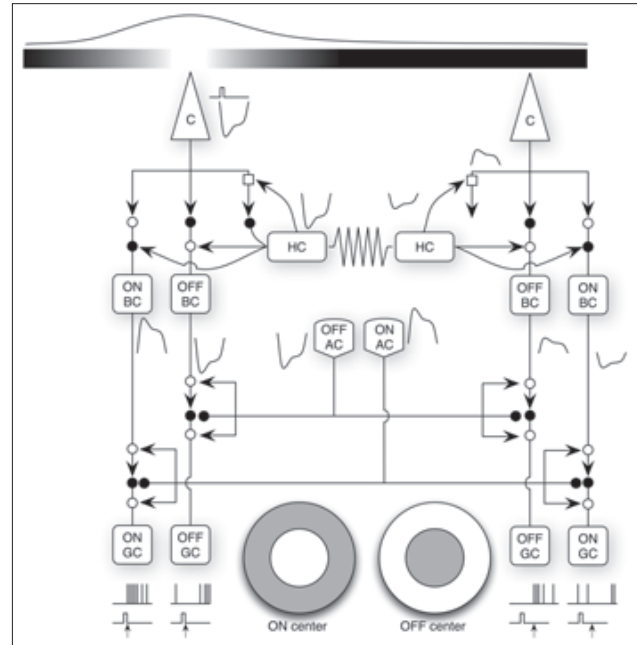


**FIGURE 122.5.** GC center-surround receptive fields. GCs at the left view a brief light pulse (white band, elevated profile) in their receptive field centers. This elicits a hyperpolarizing voltage in illuminated cones and connected OFF BCs and HCs via sign-conserving synapses (●); mGluR6 receptors invert (○) the signal in ON BCs, producing a depolarization. ON BCs synaptically depolarize ON GCs and elicit spiking. Concurrently, OFF BCs synaptically hyperpolarize OFF GCs and inhibit spiking. GCs at the right view a brief light pulse in their receptive field surrounds. Responses from distant cones propagate decrementally through the HC layer and reach nonilluminated center cones and their connected BCs. Sign-inverting HC → cone and HC → OFF BC signals lead to a small depolarization in OFF BCs; sign-conserving HC → OFF BC signals lead to a small hyperpolarization in ON BCs. Thus HCs create opponent surrounds in BCs. These are passed directly to GCs, so that surround light, with a small delay (arrows), excites OFF GCs and inhibits ON GCs. Matched ACs mediate the same pattern of surround signals in the IPL. In summary, bright centers and dark surrounds excite ON center cells, while dark centers and bright surrounds excite OFF center cells.

© REM 2006.

whereas G–G pairs are common.<sup>53</sup> Similarly, red and green cones are coupled extensively in macaque.<sup>54</sup>

## BCS – STAGE 2 OF THE VERTICAL CHANNEL

Primates display at least 10 distinct BC classes (Figs 122.9 and 122.10).

- dB1 cone BCs (OFF) may contact all cones and express KA/AMPA receptors
- dB2 cone BCs (OFF) may contact only red/green cones and express KA receptors
- dB3 cone BCs (OFF) may contact all cone classes and express AMPA receptors
- OFF midget BCs contact red, green, or blue cones and express KA/AMPA receptors
- dB4 cone BCs (ON) seem to contact all cone classes and express mGluR6 receptors
- dB5 cone BCs (ON) seem to contact all cone classes and express mGluR6 receptors
- dB6 cone BCs (ON) seem to contact all cone classes and express mGluR6 receptors



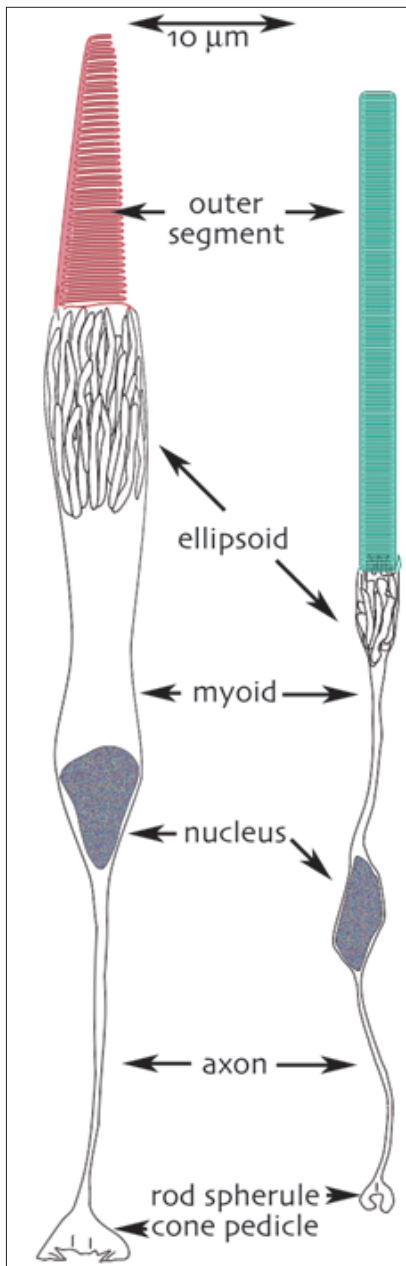


**FIGURE 122.6.** Generic photoreceptors from vertebrates with large rod-cone dimorphisms (e.g., primates). Broad outer segments, ellipsoids and myoids both a larger entrance pupil and higher metabolic and protein synthesis capacity in cones compared to rods. Large cone nuclei are located in a layer just proximal to the ELM, while rod nuclei are diversely positioned throughout the ONL. Thick cone and thin rod axons terminate in unique synaptic terminal shapes. Rod spherules contain one or two synaptic ribbons and contact ~1–2 HCs and 4–5 BCs, while cone pedicles contain ~10 ribbon and contact 50–100 BC and HC processes. © REM 2006.

- ON midget BCs contact either red or green cones and express mGluR6 receptors
- Blue cone BCs (ON) contact blue cones and express the mGluR6 receptor
- Rod BCs (ON) contact only rods and express the mGluR6 receptor

BC cells effectively copy photoreceptor signals, mix cone channels, and produce the essential functional dichotomy of all vertebrate retinas: ON and OFF channels.<sup>4</sup> ON BCs respond to light onset with sustained nonspiking depolarizations,<sup>45</sup> display long axons that extend deep into the proximal half of the IPL (known as sublamina b) and slender invaginating dendrites that preferentially terminate near the synaptic ribbons of rod and cone photoreceptors.<sup>18,56–58</sup> OFF BCs respond to light onset with sustained nonspiking hyperpolarizations, display short axons

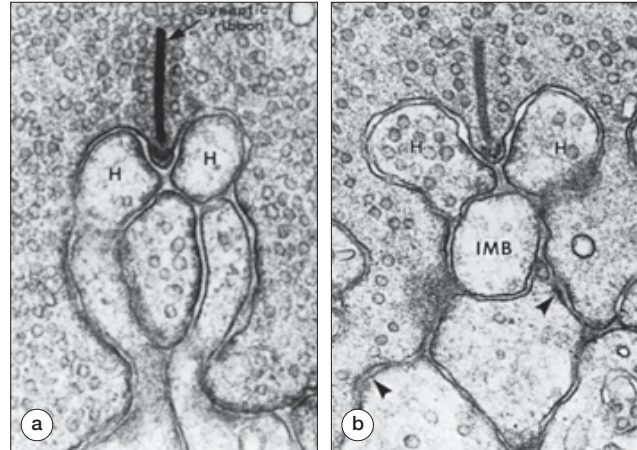


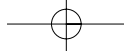
**FIGURE 122.7.** Electron micrographs of rod and cone synapses with HC and BC processes. Left, The invaginating synapse of a rod spherule. The rod vesicle fusion apparatus is composed of a synaptic ribbon that organizes vesicles for release at active zones located on either side of the dense protuberance known as the synaptic ridge. Opposite each face of the synaptic ridge are HC axon terminal processes (H). Right, An invaginating synapse of a cone pedicle containing two lateral HC dendrites (H) and the dendrite of an invaginating midget ON BC (IMB). The arrowheads show basal contacts between the cone pedicle and the dendrites of flat contact with OFF BCs. Each vesicle is ~25–30 nm in diameter. From Fawcett DW: Bloom and Fawcett: a textbook of histology. 11th edn. Philadelphia: WB Saunders; 1986.

that extend into the distal half of the IPL (known as sublamina a) and either short flat-contact or semiinvaginating dendrites that preferentially terminate further from the synaptic ribbons of cone photoreceptors (Figs 122.7 and 122.9).<sup>59</sup> In general, cone BCs are thought not to be part of the direct rod-driven path but there is now evidence that nonprimate OFF cone BCs do make sparse OFF-like contacts at rod spherules.<sup>18,60</sup> This will be reviewed in more detail later.

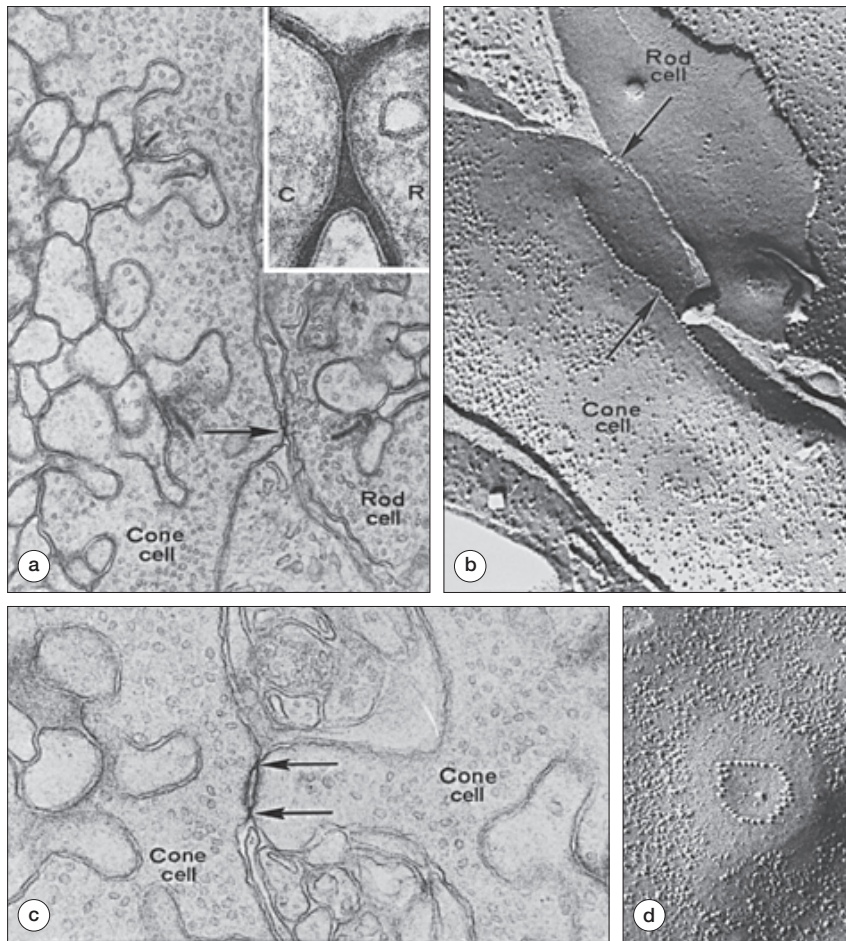
The final patterns and mechanisms of selectivity among BCs have not been fully resolved, but we have broad models for most classes (Fig. 122.11). For example, it appears that most OFF BCs will contact any cone class and midget OFF BCs exist for red, green and blue cones.<sup>61</sup> The presence of a midget blue pathway is puzzling, as chromatic aberration should blur blue targets when optimally focused for long-wave targets. It has been established that the ground squirrel homolog (squirrel type b3 OFF BC) to the primate dB2 BC selectively avoids contact with blue cones, making it an LWS cone-driven cell.<sup>62</sup> This will be presumed to be true for primates as well. As far as is known, other diffuse cone BCs are not selective and contact all cone classes. The exceptions are the blue cone ON BC that has sparse dendrites and avoids all red and green cones<sup>26</sup> and, apparently, midget ON BCs that avoid blue cones.<sup>61</sup> The mechanisms that guide selective contacts are unknown and could involve paired-cell adhesion and recognition mechanisms or competition for synaptic targets, or both. On balance, it is clear that rods and blue cones are either targeted or avoided, suggesting that their synaptic terminals represent distinct chromatypes. There is no evidence that any postsynaptic cell can discriminate red and green cones terminals.

The ultrastructural patterns of contacts are specialized by class. Most ON BCs tend to generate slender invaginating dendritic tips that form a narrow adhesion en passant contacts with cone membrane and terminate in a so-called central position (Fig. 122.7) in a triad of processes near the synaptic

AU:  
Do figures  
1-18 and  
20-24  
require  
permission?  
If so, please  
supply  
relevant  
correspon-  
dences  
granting  
permission.



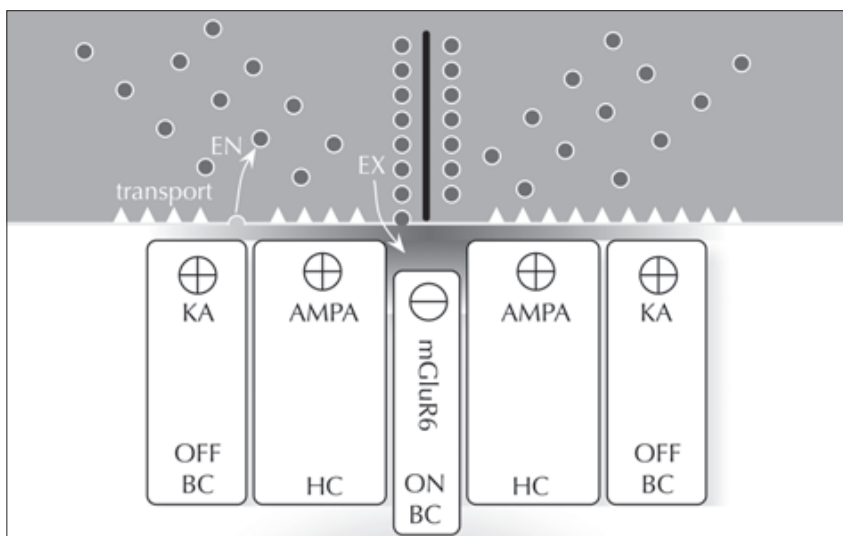
## RETINA AND VITREOUS



**FIGURE 122.8.** Gap junctions between photoreceptor pairs in the primate retina. **(a)** A cone pedicle and a rod spherule coupled by a punctate junction (arrow). Inset, At higher magnification with lanthanum tracer in the intercellular space the junction is characterized by a focal apposition of the adjoining extracellular leaflets of the two plasma membranes. C, cone; R, rod. **(b)** Freeze fracture imaging shows that such focal appositions represent the fortuitous cross section of a linear array of connexons. **(c and d)**, A pair of cone pedicles connected by gap junctions (arrows) that consist of a circular array of connexons. Scaling for transmission images: each vesicle is ~25–30 nm in diameter. Scaling for freeze fracture images: each connexon is ~6.5 nm in diameter.

From Raviola E, Gilula NB: Gap junctions between photoreceptor cells in the vertebrate retina. *Proc Natl Acad Sci USA* 1973; 70:1677.

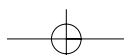
AU: Please supply last page number for all journal type references, if available.



**FIGURE 122.9.** Topologically simplified vesicle fusion and glutamate diffusion patterns around a single cone synaptic ribbon (thick black line in the gray box). Vesicles loaded with high levels of glutamate (dark gray) fuse with the cone membrane (EX) at active zones on either side of the synaptic ribbon and are recovered from sites displaced from the ribbon (EN). HCs expressing sign-conserving (+) AMPA receptors are likely closest to sites of vesicle fusion. ON BCs expressing sign-inverting (–) mGluR6 receptors are centered under the ribbon but are slightly displaced from fusion sites. OFF BCs expressing sign-conserving (+) KA receptors are most distant from vesicle fusion sites. Alternatively, HCs and OFF BCs are closest to cone glutamate transporters that remove glutamate from the cleft. The glutamate released into the cleft is progressively cleared as it diffuses from the ribbon. Thus OFF BC receptors likely sense a much lower mean glutamate level. © REM 2006.

ribbons of photoreceptors.<sup>48,56–58</sup> This means that ON BC mGluR6 receptors are positioned close to the source of vesicle fusion and experience a relatively high mean glutamate level, modulated by cone voltage-dependent increases and decreases in release and clearance.<sup>18</sup> This is consistent with the modest

glutamate sensitivity of the mGluR6 receptor.<sup>3</sup> Conversely, most OFF BCs tend to generate blunt 'flat' dendritic tips that form wide adhesion contacts with the cone plasmalemma and terminate in a position distant from the synaptic ribbons of photoreceptors (Figs 122.7 and 122.9). This means that OFF





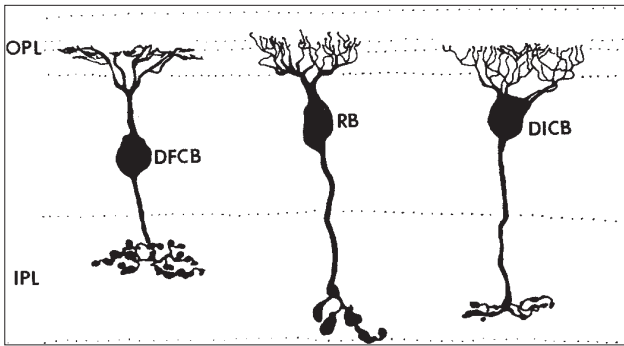


**FIGURE 122.10.** Three diffuse BC classes from Rhesus monkey retina, visualized by the Golgi technique. At left, one of the OFF cone BC classes (diffuse flat cone bipolar or DFCB) makes flat contacts with cones in the OPL and has a broadly stratified terminal in sublamina a of the IPL. At center, an ON rod BC (RB) makes invaginating ribbon contacts with cones in the OPL and has a varicose terminal in sublamina c of the IPL. At right, one of the ON cone BC classes (diffuse invaginating cone bipolar or DICB) generates invaginating ribbon contacts with cones in the OPL and has a narrowly stratified terminal in sublamina b of the IPL.

From Mariani AP: a diffuse, invaginating cone bipolar cell in primate retina. *J Comp Neurol* 1981; 197:661.

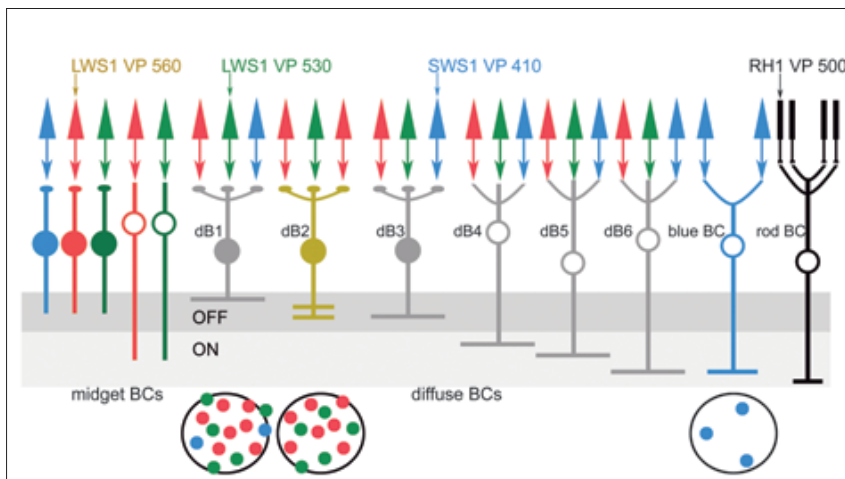


**FIGURE 122.11.** A summary of ten BC classes and their connections in the trichromatic primate retina. (Class 1) Three short OFF midget BCs terminate in the OFF sublayer. (Class 2) Two long ON midget BCs terminate in the ON sublayer. (Classes 3–5) Three diffuse OFF cone BCs with flat contacts terminate in different levels of the OFF sublayer. Classes dB1 and dB3 have narrow terminal stratifications and may contact all cone classes. Class dB2 has a broadly stratified terminal and may contact only R and G cones. (Classes 6–8) Three diffuse ON cone BCs with invaginating contacts terminate in different levels of the ON sublayer. (Class 9) Blue BCs contact B cones with invaginating contacts and terminate deep in the ON sublayer. (Class 10) Rod BCs contact rods with invaginating contacts and have the deepest terminals in the ON sublayer. The circles indicate representative cone contact patterns for dB1, dB2, and blue BCs.

© REM 2006.

BC iGluR receptors are positioned farther from the source of vesicle fusion, experience a lower mean glutamate level modulated by cone voltage-dependent increases and decreases in release and clearance.<sup>3</sup> This is consistent with the relatively high glutamate sensitivity of the KA receptor found on subsets of OFF BCs.<sup>63–65</sup> On an intermediate scale, some OFF BCs are known to invaginate some dendrites much closer to the ribbon than those that make flat contacts<sup>59</sup> and these invaginating OFF BCs express AMPA receptors.<sup>65</sup> The fluctuations in glutamate levels are also faster near the ribbon and smoothed at flat contacts, suggesting that KA and AMPA receptors represent key temporal filters for BCs.<sup>65</sup> The complex topology of this arrangement of processes is represented in a simplified two-dimensional form (Fig. 122.9).

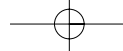
BC outputs, like those of photoreceptors, are restricted to the axon terminal specialization of the basal pole of the cell (Fig. 122.12). Again, like photoreceptors, BCs utilize synaptic ribbons to facilitate high rates of vesicle release. The ribbons are generally smaller than rod and cone ribbons and quite numerous, with each BC having from many small synaptic ridges, each targeting a pair of postsynaptic AC dendrites or, less frequently, a GC-AC pair. BC synaptic terminals tend to be (1) lobular and branched in a local cluster of small telodendria (midget, rod, and blue BCs) with a lateral spread similar to the diameter of the soma or (2) filamentous and branched in a pattern resembling the dendritic arbor in shape and extent. Thus some BCs provide output to only a few target cells and preserve a narrow receptive field structure, while others branch to reach many targets, facilitating a divergence of signals.

The axon terminals of BCs are the vertical structuring elements of the IPL. OFF BCs terminate in the distal half (sublamina a) and ON BCs in the proximal half (sublamina b) (classical refs). The late Brian Boycott pointed out that the deep proximal IPL where rod BCs drive rod ACs is structurally unique and he proposed it to be sublayer c.<sup>66</sup> Each AC and GC thus sends its dendrites to specific levels of the IPL where the specific BCs are sampled. GCs targeting sublamina a or b are respectively dominated by OFF or ON BCs, while those whose dendrites span both sublayers typically show mixed ON–OFF behavior.<sup>45</sup> It has long been common to separate the IPL into five sublayers, though there is no biological basis for the practice. Indeed, various immunochemical markers show that the mammalian IPL can be segmented into no fewer than seven sublayers and nonmammalian retinas easily possess up to 15 sublayers.<sup>3</sup> The best practice is to specify the level of the IPL by setting the ACL/IPL border at 0 and the GCL/IPL border at 100.

### GCS—STAGE 3 OF THE VERTICAL CHANNEL

Mammals display at least 15 distinct GC classes (Figs 122.13 and 122.14).

The diversity of mammalian retinal GCs has been assessed by Golgi impregnation, dye labeling, transgene expression and molecular phenotyping strategies.<sup>42,43,67–71</sup> The exact numbers are not known but clearly exceed 15 and may even exceed 20,<sup>68,70</sup> even in primates. Exact homologies have not been established across mammals, but there are some basic commonalities of structure. Nearly all GCs have their somas in the GC layer



## RETINA AND VITREOUS

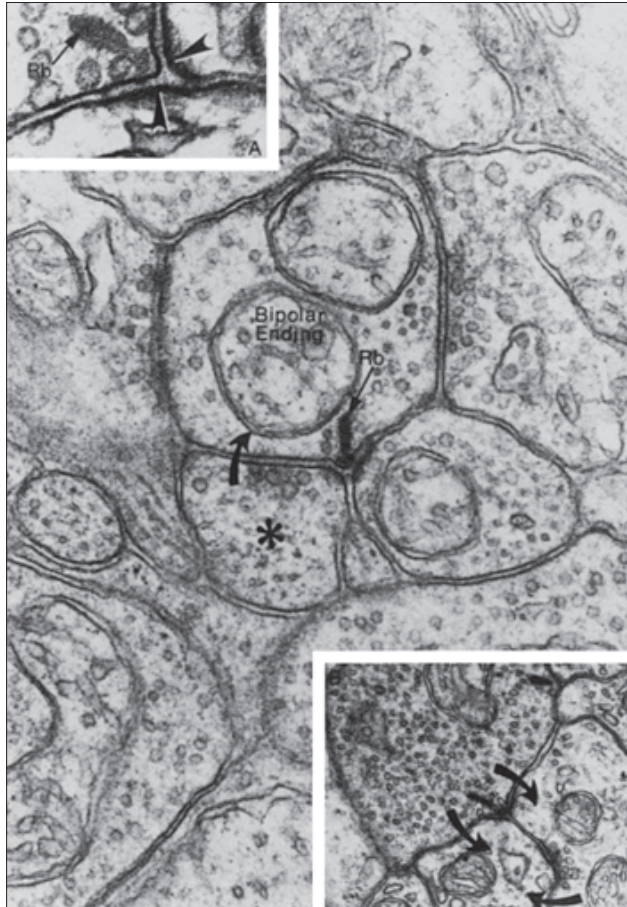


**FIGURE 122.12.** Cone BC synaptic terminals in the mammalian IPL. BC ribbon synapses generally target two postsynaptic processes in dyad synapse. In this instance, both postsynaptic processes are AC dendrites, one of which (asterisk) makes a conventional reciprocal feedback synapse (curved arrow) with the BC. Another AC synapses on the BC the right margin of the terminal. Rb, synaptic ribbon; primate retina. Inset upper left, A ribbon synapse at higher magnification showing the pentalaminar ribbon structure, a halo of synaptic vesicles, enlarged synaptic cleft, postsynaptic densities in the target cells (arrowheads). Rabbit retina. Inset lower right, a BC → AC → GC feedforward chain. The curved arrows indicate the direction of signaling. Primate retina. Scaling for transmission images: each vesicle is ~25–30 nm in diameter.

From Raviola E, Raviola G: Structure of the synaptic membranes in the inner plexiform layer of the retina: a freeze fracture study in monkeys and rabbits. *J Comp Neurol* 1982; 209:233.

proper and exhibit a variety of dendritic patterns, ranging from compact narrow-field to highly branched wide-field, with laminar patterns ranging from narrowly stratified to bistratified and ultimately to diffuse laminations. In the primate retina, several GC classes have been studied described anatomically and physiologically.

- Midget GCs (OFF) contact OFF midget BCs
- Midget GCs (ON) contact ON midget BCs
- Large bistratified blue ON GCs contact blue BCs and OFF bB2-like BCs
- Small bistratified blue ON GCs contact blue BCs and OFF bB2-like BCs
- Parasol GCs (OFF) contact diffuse OFF BCs (likely dB3)
- Parasol GCs (ON) contact diffuse ON BCs (likely dB4)
- Inner giant melanopsin GCs contact diffuse ON BCs (likely dB6)
- Outer giant melanopsin GCs contact unknown cell classes

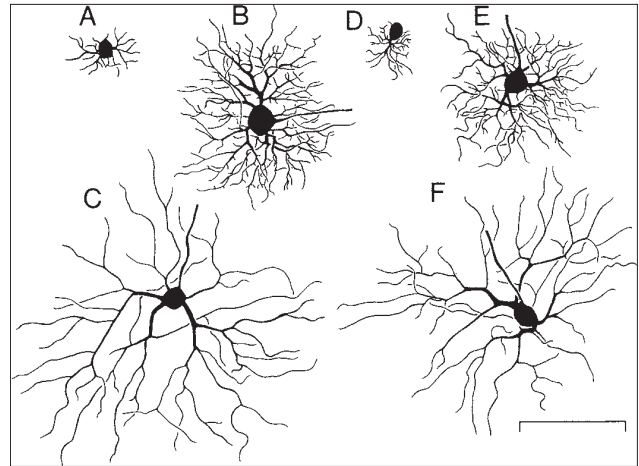


**FIGURE 122.14.** A horizontal plane view of medium-field class  $\beta$  ON center (A, B, C) and OFF center (D, E, F) GCs of cat retina visualized with the Golgi technique. Cells A and D are near the *area centralis*, cells B and E from the near periphery, and cells C and F from the periphery at 9 mm eccentricity (~40°). All are the same class of cell with graded field diameters reflecting changes in cone density. Bar = 100  $\mu$ m.

From Wässle H, Boycott BB, Illing RB: Morphology and mosaic of on and off beta cells in the cat retina and some functional considerations. *Proc R Soc Lond [B]* 1981; 212:177.

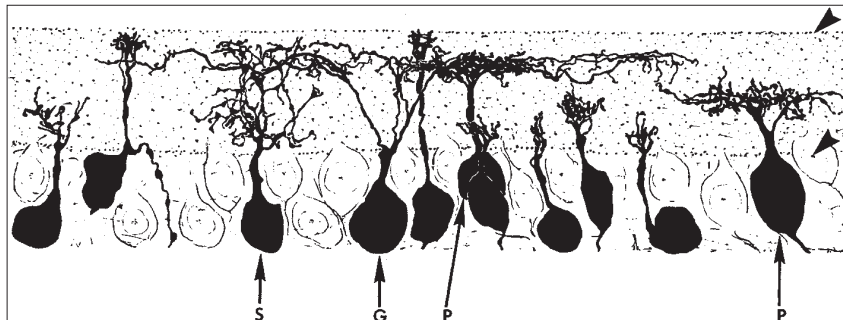


**FIGURE 122.13.** Primate narrow-field midget, medium field parasol and wide-field garland GCs visualized with the Golgi technique and labeled according to Steven Polyak's 1941 classification. Two different parasol GCs (P) send their dendritic arbors to the distal OFF and proximal ON sublayers of the IPL, as do several midget GCs (unlabeled). A shrub GC (S) appears to have a small diffusely bistratified arbor. A garland GC (G) arborizes widely in the OFF sublayer. The arrowheads denotes the IPL borders.

Modified from Polyak SL: *The retina*. Chicago: University of Chicago Press; 1941.

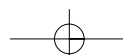




**TABLE 122.3. Provisional Functional and Anatomical Assignments of Mammalian GCs**

Physiology	MacNeil/Marc/Famiglietti Class (Coupling), Percent	Structural Features, Level	Primate Homologs
<b>Concentric Brisk Linear</b>			
ON sustained X, $\beta$	G4 / 3 / IIa, 12.2%	Medium monostratified, 35–45	ON midget
OFF sustained X, $\beta$	G4 / 6 / IIb1 ( $\gamma$ ), 15%	Medium monostratified, 55–65	OFF midget
ON transient	G? / 1b	Medium monostratified, 35–45	ON parasol?
OFF transient	G? / 5 ( $\gamma$ )	Medium monostratified, 35–45	OFF parasol?
<b>Concentric Brisk Nonlinear</b>			
ON transient Y, $\alpha$	G11 / 1a / Ia2, 2.8%	Wide monostratified, 60–80	?
OFF transient Y, $\alpha$	G11 / 9 / Ib2 ( $\gamma$ ), 1.4%	Wide monostratified, 30–40	?
<b>Concentric Sluggish Linear</b>			
ON sluggish sustained	G? / 2, 4.2%		?
OFF sluggish sustained	G? / 8 ( $\gamma$ ), 12.2%		?
<b>Concentric Sluggish Nonlinear</b>			
ON + OFF sluggish transient	G? / 12 ( $\gamma$ ), 5.2%		?
<b>Complex</b>			
Local edge detector	G1 / 7 ( $\gamma$ G), 5.6%	Narrow monostratified, 50	?
Uniformity detector	G6 / 5 ( $\gamma$ ) or 1b?	Medium monostratified, 80	Melanopsin GC ?
Orientation selective	G? / 11 ( $\gamma$ ), 6.6%		?
ON-OFF DS	G7 / 1c & 10 ( $\gamma$ )	Wide bistratified, 25 and 75	?
ON DS	G10 / 4, 7.7%	Medium monostratified, 70–80	?
Blue ON Green OFF	G3 ? / ?	Medium bistratified, 20 and 80	Blue ON Yellow OFF

GC populations in cat and rabbit retina have been analyzed more comprehensively and, based on several recent studies can be parsed into at least a dozen clear structural, molecular, and physiological categories (Table 122.3 and Table 122.4).

Narrow-field GCs, such as midget GCs (Fig. 122.13), are monostratified cells with medium-sized somas that selectively contact the axon terminals of midget BCs, and are ON or OFF cells.<sup>45</sup> Such cells typically generate relatively sustained spiking patterns to a maintained light stimulus. In the foveola each midget GC contacts a single midget BC but midget GCs may contact several midget BCs in peripheral retina.<sup>72,73</sup> Midget GCs project to the dorsal parvocellular (small cell) P layers of the LGN that in turn project to layer 4C $\beta$  of striate visual cortex area V1.<sup>74</sup> Projection neurons along parvocellular retina  $\rightarrow$  LGN  $\rightarrow$  cortex stream appear to be key elements in high-acuity

vision, and tend to have sustained responses. Their roles in hue discrimination have been debated, but it is likely that the essential information for hue discrimination is embedded in their signals.<sup>1</sup> As they share some morphological features, functions and projections, primate<sup>74</sup> and ground squirrel midget GCs,<sup>75</sup>  $\beta$  cells of the cat retina<sup>76</sup> and classes 3 (IIb2) and 6 (IIa) GCs of rabbit<sup>42,67</sup> are likely homologs. Species differences in GC morphology are partly due to variations in cone density and patterning. In trichromatic primates, midget cells are thought to generate the VP 560-driven and VP 530-driven ON and OFF sustained GCs that may subserve red-green hue discrimination. However, just as midget BCs likely do not discriminate between red and green cones, parafoveal midget GCs that collect signals from a few midget BCs do not appear to have any color selectivity<sup>1,77</sup> and lack color opponency.<sup>73</sup>

Medium to wide-field GCs (Fig. 122.13) are the most common types in most retinas but likely represent mixed functional classes. One distinctive class in most species is a medium-density to sparse population of large somas with very large dendritic arbors, such as parasol GCs in primates and  $\alpha$  or  $\alpha$ -like cells in other mammals. These cells sharply stratify their dendrites at specific levels of the IPL, suggesting that they preferentially sample from cells such as OFF dB2/3 BCs<sup>78</sup> or ON dB4/5 BCs. Parasol GCs preferentially project to the ventral magnocellular (large cell) or M layers of the LGN, thence to layer 4C $\alpha$  of striate visual cortex area V1<sup>79</sup> and are achromatic or luminance-driven neurons. In cat and rabbit, such cells show transient responses; brief bursts of spikes to a step of light at light onset (ON cells) or offset (OFF cells).<sup>45</sup> However, the presumed parasol GCs of primate retina and most LGN magnocellular neurons are rather linear in their responses<sup>79</sup> and may not be true  $\alpha$  homologs, or may be a re-derived variant

**TABLE 122.4. Optical Sampling Across Species**

Species	Visual Angle in ( $\mu$ m/deg)
Human	280–300
Macaque	246
Cat	220
Rabbit	160–180
Rat	75
Goldfish	60
Mouse	31
Zebrafish	10 (estimated)

## RETINA AND VITREOUS

(e.g., progenitor duplication instead of gene duplication). Large sparse GCs with even larger dendritic arbors are plausibly the primate  $\alpha$  OFF cell.<sup>69,70</sup>

Bistratified GCs arborize in both sublayers of the IPL, giving them the opportunity to capture signals from BCs with opposite polarities. There are several known examples, but the attributes of none are known particularly well. In cat, ON-OFF transient cells resemble bistratified  $\alpha$  cells. In rabbit, a set of GCs sample from sublamina a and b near the midline of the IPL and generate independent ON and OFF directionally selective (DS) responses. ON-OFF DS cells are one of the most complex neurons known and, though their receptive field mechanisms have been studied intensively, the underlying biological basis of its tuning remains controversial.<sup>80</sup> DS cells have not been studied thoroughly in primates, but the ACs most often associated with them are present in primates<sup>81</sup> and likely candidates for both monostратified ON DS and bistratified ON-OFF DS cells have recently been described in macaque.<sup>70</sup> The most distinctive primate small-field bistratified cell is the blue ON bistratified GC that collects inputs from a diffuse OFF BC (likely dB2) and blue ON BCs. Thus the receptive field center of this cell is spectrally biphasic, depolarizing and spiking to blue light and hyperpolarizing to yellow light.<sup>82</sup>

Melanopsin GCs in primate are 'giant' GCs that narrowly stratify at the proximal or distal margins of the primate retina.<sup>83</sup> Some giant melanopsin GCs appear misplaced or displaced to the ACL. Melanopsin GCs (also known as intrinsically photosensitive or ipGCs) are present in other mammals,<sup>84–86</sup> project widely in the thalamus and pretectum, and partly drive the pupillary response.<sup>87</sup> In primates, these cells appear to be the rare blue OFF/yellow ON (B-/Y+) GCs of the retina.<sup>87</sup> In addition to a full range of rod and cone responses, these cells express melanopsin, a photosensitive GPCR that uses 11-cis retinaldehyde as a chromophore.<sup>88</sup> At high photopic levels, melanopsin directly drives highly sustained spiking activity, partially compensating for the transient nature of cone-driven responses.<sup>83</sup> Melanopsin GCs in many species project to the suprachiasmatic nucleus (SCN) as part of the circadian clock pathway and to the olivary pretectal complex as part of the pupillary response pathway. In primates they also project to the LGN.<sup>83</sup> Evidence is building for the existing of several subclasses of melanopsin GCs.<sup>86</sup> Most importantly, these cells likely underlie the persistence of photic entrainment of circadian cycles, even after photoreceptor degeneration.<sup>89,90</sup>

GCs are purely postsynaptic neurons from a neurochemical perspective, and decode BC signals with a mixture of AMPA and NMDA receptor subtypes.<sup>3,42,91,92</sup> AC signals are decoded with a variety of GABA and glycine receptors.<sup>6</sup> GC dendrites make no presynaptic contacts and are thought to be entirely postsynaptic. However, some GC classes make heterocellular gap junctions with ACs, forming specific GC::AC::GC syncytia.<sup>8,42,93,94</sup> Each retinal GC generates a single unmyelinated axon that becomes myelinated in the optic nerve and projects to one or more CNS targets: LGN, SCN, pretectum, and superior colliculus.

### HCS – THE LATERAL CHANNEL FOR PHOTORECEPTOR → BC SIGNALING

Every GC is a logical device that compares vertical channel signals with those from several lateral channels. There are at least two formal lateral channel topologies in the OPL:

- cone<sub>1</sub> → HC → cone<sub>1</sub> reciprocal feedback (temporal)
- cone<sub>1</sub> → HC → cone<sub>2</sub> lateral feedback (spatial, spectral)
- cone → HC → BC lateral feedforward (temporal, spatial, spectral)

These chains partly shape GC responses that encode contrast, color, and spatial timing of natural stimuli. A general engineering principle states that each step of high gain (photoreceptor or BC ribbon synapses) requires a stabilizing negative feedback element.<sup>95</sup> The quantitative differences between feedback and feedforward are beyond the scope of this chapter. HCs are the lateral processing elements of the OPL and enable BCs to compare direct light signals captured by photoreceptors they contact and indirect light signals from surrounding photoreceptors they do not. Neither the mechanisms of HC signaling or the relative strengths of the cone → HC → cone lateral feedback and the cone → HC → BC lateral feedforward paths are known though several models exist.<sup>3</sup>

Topologically, HCs exhibit two forms in mammals; axon-bearing and axonless.<sup>96–99</sup> All HCs contact cones with their dendritic arbors while axon-bearing HCs form large axon terminal arbors that contact rods (Fig. 122.15).<sup>99</sup> Many mammalian species display both, while rodents apparently

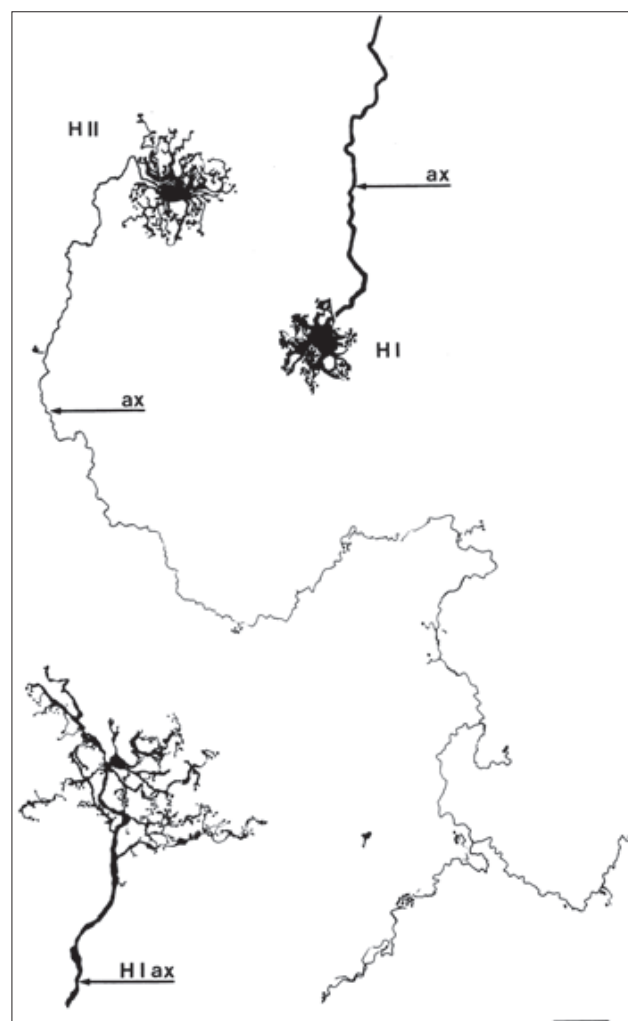


**FIGURE 122.15.** A horizontal plane view of H1 (HI) and H2 (HII) HCs from the macaque visualized with the Golgi technique. ax, axon. Bar = 15  $\mu$ m.

*Slightly modified from Kolb H, Mariani A, Gallego A: A second type of horizontal cell in the monkey retina. J Comp Neurol 1980; 189:31. Copyright © 1994 John Wiley & Sons.*

develop only a single class of axon-bearing cells.<sup>100</sup> No evidence exists to support the idea that the axons of mammalian HCs are electrically functional.<sup>101</sup> HCs do not generate action potentials and the somatic and axon terminal fields respectively generate cone-selective and rod-selective light responses with no evidence of signal mixing that can be attributed to the axon. Indeed we might consider an axon-bearing HC to be two separate cells that share a single nucleus. The primate retina is more complex than any other mammal as it likely harbors three HC classes.<sup>101–104</sup>

- H1 HC somatic dendrites contact all cones and lack axons in the rod-free foveola
- H1 HC responses indicate dominance by R and G cone inputs
- H1 HC axon terminals contact rods
- H2 HC somatic dendrites appear to contact all cone classes, with a blue cone bias
- H2 HC axon terminals appear to contact all cones, with a blue cone bias
- H3 HC somatic dendrites contact cones, apparently avoiding blue cones
- H3 HC axon terminals contact rods

AU: Please clarify the respective ratios.

H1 and H2 HCs are the most abundant classes, with an H1:H2 ratio of 4 in the fovea.<sup>105</sup> H3 HCs have been described only in Golgi preparations and have been difficult to document. But Golgi studies have rarely been incorrect and so the search for the H3 cell by molecular means continues. The somas of primate HCs and mammalian axon-bearing HCs are ovoid and give rise to 8–12 dendrites that ultimately contact ~12 cones in the foveola and 20 cones in the periphery. The axons contact a few hundred rods in primates and many more in cat. Though primate H1 somas appear to contact all cones, they clearly have responses dominated by R and G cones, with little B input.<sup>106–108</sup> Conversely H2 HCs are enriched in blue responses, reflecting their tendency to contact a disproportionate number of blue cones.<sup>108</sup> Axon terminals have rod-driven responses.

The processes of both HC somas and axon terminals are dendritic in nature. The dendrites are lobular and flank the synaptic ridges of photoreceptors as lateral elements of a synaptic triad (Fig. 122.7).<sup>99</sup> The dendrites are thus close to the sites of photoreceptor vesicle fusion. HCs express AMPA receptors,<sup>3,91,109,110</sup> but the precise locations of the functional receptor patches are not certain. Since geometric factors such as the spatial coherence of vesicle release and the distribution of glutamate transporters along the diffusion path, the precise receptor position is a key datum.

While HCs are clearly postsynaptic to photoreceptors, it has been extremely difficult to discover their outputs. This issue has been treated extensively elsewhere,<sup>3,18</sup> but classical presynaptic specializations are missing in HCs. Presence of GABA in some mammalian HCs has led to the view that they must be GABAergic, though compelling demonstrations of that fact are few. Wilson<sup>39</sup> provides a comprehensive and insightful review of these issues. However, there are many mammalian HCs that completely lack any evidence of GABA content. Further, there is no evidence for transporter-mediated export found in nonmammals. Physiological studies in nonmammals imply that there is no feedback path from HCs to rods but there is to cones. Paradoxically, vesicles similar to classical synaptic vesicles are more common in HC dendrites contracting rod spherules than those contacting cone pedicles,<sup>111</sup> but there is no obvious conventional presynaptic assembly and no evidence of stimulated fast exocytosis or endocytosis in HC dendrites. Indeed, similar dendritic accumulations of vesicles in brain neurons appear to be involved in the regulated cytoskeletal

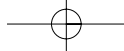
delivery and turnover of postsynaptic AMPA receptors to dendrites as vesicular cargo.<sup>112</sup> HC dendrites have also been argued to serve as ephaptic feedback devices via patches of hemijunctions (arrays of half-connexins) through which currents leak constitutively.<sup>7</sup> In fishes, connexin26 hemijunctions are very close to the voltage-sensitive  $\text{Ca}^{2+}$  channels that regulate cone vesicle fusion.<sup>113</sup> When the HC layer is hyperpolarized by closure of AMPA receptor channels, the focal inward current through hemijunctions makes the local intrasynaptic potential more negative than the adjacent intracellular cone potential and this relative depolarization is perhaps sensed by cone  $\text{Ca}^{2+}$  channels which begin to open, increasing transmitter release briefly. This feedback effect requires no transmitter-dependent or vesicle mechanism, which nicely explains why many HCs contain no measurable inhibitory transmitter, yet apparently function quite effectively.

Finally, HCs somas are strongly coupled to each other by large dendritic gap junctions, so that synaptic currents generated by cones spread readily in the HC layer.<sup>101</sup> In nonprimates such as rabbits, axonless HCs are more strongly coupled than the far more abundant axon-bearing HCs.<sup>114,115</sup> This generates two distinct spatial classes of HCs, though the functional significance of this dichotomy remains unknown. Coupling efficacy of axon-bearing primate H1 cells coupling resembles the weak coupling of rabbit axon-bearing coupling.<sup>116</sup> H1 and H2 cells form separate coupled mosaics.<sup>105</sup>

### ACS – LATERAL CHANNELS FOR BC → GC SIGNALING

- BC → AC → BC reciprocal lateral feedback
- BC1 → AC → BC2 lateral feedback
- BC → AC → GC lateral feedforward
- AC → AC concatenated feedforward chains

ACs are the most diverse group of neurons in the retina,<sup>8</sup> with over 70 classes in teleost fishes<sup>117</sup> and over 25 classes in mammals.<sup>44</sup> Most ACs, by definition, lack classical axons and function as local circuit neurons via dendritic synapses, usually as negative feedback and feedforward control elements. While a precise tally is still uncertain, about two-third of AC classes appear GABAergic, with the rest glycinergic. Other candidate AC transmitters often co-localize with GABA.<sup>3</sup> ACs exhibit diverse morphologies with lateral spread of dendrites ranging from narrow (<100  $\mu\text{m}$ ) through medium (100–200  $\mu\text{m}$ ) to wide (>200  $\mu\text{m}$ , with some cells > 1 mm) based on a comprehensive study of rabbit ACs.<sup>44</sup> Narrow-field cells such as the classic glycinergic rod (AII) AC (Fig. 122.16) typifies many narrowly stratified, bistratified, and diffusely arborized classes.<sup>15–17,118</sup> Most medium-field cells have diffuse arbors while most wide-field cells such as GABAergic starburst ACs (Fig. 122.17) are narrowly stratified.<sup>120,121</sup> Similarly, the wide-field type S1 and S1 GABAergic rod ACs (also known as A17, AI, and indoleamine-accumulating ACs), appear to have very diffuse arbors but, in reality have most of their inputs and outputs very narrowly stratified within sublayer c at ~90–100 level of the IPL.<sup>68,122–125</sup> Thus there are two broad signaling motifs of importance; narrowly stratified and usually GABAergic ACs provide lateral signals within a set of BCs and their targets, while diffuse (often glycinergic) ACs provide lateral signals across different sets of BCs and their targets. As there are at least twice as many AC classes as BC and GC classes, each BC should thus drive at least two different kinds of ACs. But things are clearly more complex than this, as dendrites from at least ten different ACs arborize at any level of the IPL between 0 and 90. This emphasizes our nearly complete lack of



## RETINA AND VITREOUS

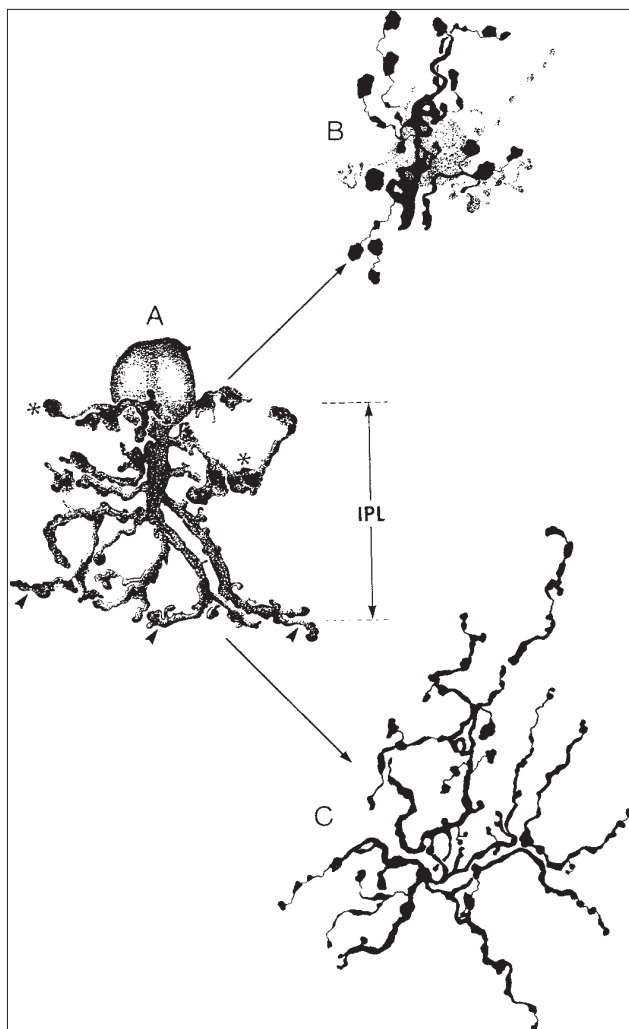


**FIGURE 122.16** A narrow-field rod AC (AII) viewed in vertical (image A) and horizontal planes in the OFF (image B) and ON (image C) sublayers of the IPL in rabbit retina. In the OFF sublayer, tortuous fine branches arise from the cell body and primary dendrite and terminate as large lobular appendages (asterisks). In ON sublayer, the primary dendrite gives rise to a conical tuft of arboreal branches that spread tangentially at the IPL–GCL border and carry small swellings (arrowheads). Image A was visualized with the Golgi technique, and images B and C are optical sections visualized by single cell dye injection. The IPL width is ~25  $\mu\text{m}$ .

Slightly modified from Dacheux RF, Raviola E: *The rod pathway in the rabbit retina: a depolarizing bipolar and amacrine cell*. *J Neurosci* 1986; 6:331.

understanding of the various inputs and outputs for any AC across levels except for one archetypal neuron; the glycinergic rod (AII) AC. This AC is actually a tristratified cell that receives rod BC input at level 90–100, makes gap junctions with cone ON cone BCs at levels 55–80 and forms inhibitory glycinergic synapses on cone OFF BCs at levels 10–35.<sup>3,16–18</sup> Many other diffuse or bistratified ACs may have similarly diverse patterns of inputs and outputs. There is an exception to this complex lamination. The proximal band at level 90–100 contains the axon terminals of rod BCs and only the arbors of only three classes of rod ACs; the narrow-field glycinergic AC and two wide-field GABAergic rod ACs.<sup>44,125</sup> This further supports the designation of this band of IPL as a unique sublayer.<sup>66</sup> One additional feature tends to correlate with signaling within

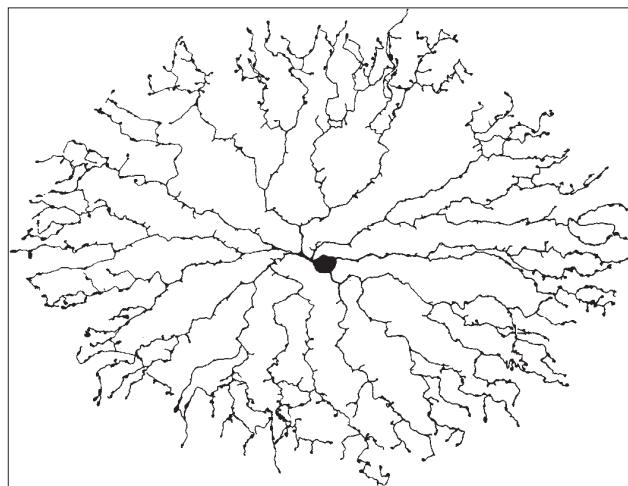
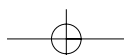


**FIGURE 122.17** A horizontal plane view of a wide-field starburst AC from the rabbit retina. Note the regular dichotomous branching of its dendrites and the concentration of endings at the periphery. Visualized by single-cell dye injection. The dendritic field is ~140  $\mu\text{m}$   $\times$  200  $\mu\text{m}$ . From Tauchi M, Masland RH: *The shape and arrangement of the cholinergic neurons in the rabbit retina*. *Proc R Soc Lond [B]* 1984; 223:101.

versus across levels and that is neurotransmitter class. Many narrowly stratified cells tend to be GABAergic and AC  $\rightarrow$  BC reciprocal synapses and the BC  $>$  AC  $>$  i BC chain are almost exclusively GABAergic.<sup>3</sup> Correspondingly, density of GABA synapses is extremely high and accounts for ~90% of the synaptic innervation in the vertebrate IPL (Fig. 122.2). Several diffuse or multistratified cells may mediate BC  $>$  gly AC  $>$  i GC or BC signaling across strata. Cholinergic signaling as mediated in mammals by the ON and OFF starburst ACs<sup>3,8,80,126</sup> which are also GABAergic neurons.<sup>3</sup> These cells are narrowly stratified and form two excitatory output systems at levels 20–25 and 65–75 of the IPL. Their presumed primary targets are DS GCs in rabbits<sup>80</sup> and DS candidate GCs have been described in macaque.<sup>81</sup> Expression patterns of AC neurotransmitters are reviewed in detail by Marc<sup>3</sup> and Brecha.<sup>37</sup>

## LARGE-SCALE PATTERNING OF RETINAL CELLS

Vertebrates with large eyes also show large-scale variations in cell density and composition of the neural retina,<sup>1</sup> likely reflecting the power of niche selection to control global tissue patterning signals (Fig. 122.18). Many species concentrate cones in retinal regions where the optical quality is high (central foveas in primates) or in horizontal streaks to represent a strong behavioral bias for horizon-related visual transitions (urodele amphibians, chelonian reptiles, lagomorph mammals). The biophysics of foveal formation are poorly understood, though Springer and Hendrickson<sup>127</sup> have argued that increased intraocular pressure and growth-induced retinal stretch induce the primate foveal pit. While these ideas do not easily explain other patterns, especially the deep convexitivates foveas of lizards or the dual and differently shaped foveas of avians that may involve both local proliferation and cell migration, they offer testable models. Developing genetic models for studying tissue sculpting in large eyes will be challenging,<sup>128</sup> although development of transgenic and knockout avians and advanced quantitative trait locus analyses may offer new ways to understand the genes that control foveal formation and global neuron patterning.





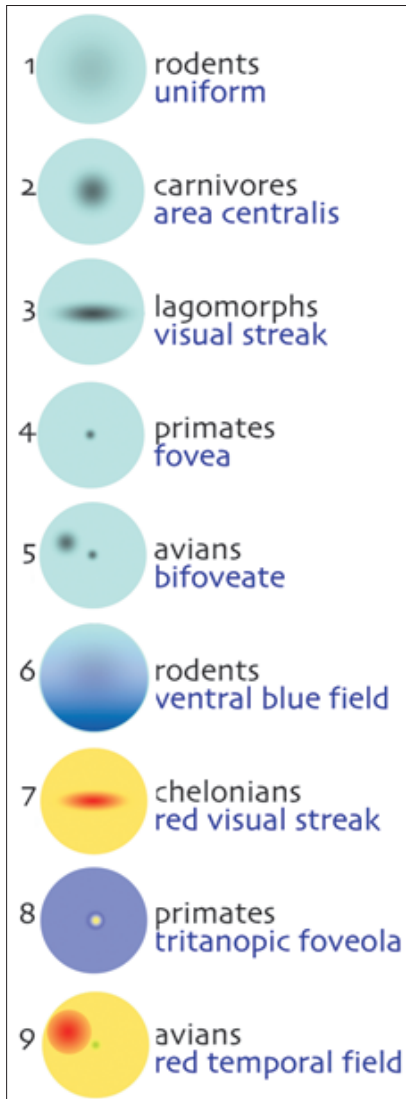


**FIGURE 12.18.** Large-scale spatial variations in cone density. (1) Most rodents display weak central elevations in cone density. (2) Carnivores have strong concentrations of cones and GCs in the central retina. (3) Prey animals such as rabbits (Lagomorpha) express distinct linear bands of high cone, BC, AC, and GC density. (4) Diurnal primates express compact, high-density, pure-cone foveas centered in a large low-density cone field. (5) Avians express the most complex density variations, with a central pure cone region exceeding primate densities and a second moderately high density region specialized for binocular vision. (6) Many rodents, such as domestic mice, display pure blue cone ventral fields. (7) Aquatic reptilians such as turtles (Chelonia) possess very high-density linear streaks (approaching primate densities) enriched in cones with red oil droplets. (8) Primates are unique among all vertebrates (as far as is known) in having a tritanopic fovea where the central 15' arc contains few or no blue cones and a peak of blue density at 0.3–1° eccentricity. (9) Finally, the bifoveate avians possess differential enhancements of cones, with high red-oil droplet cones dominating the temporal fovea and yellow oil cones dominating the central fovea and most of the peripheral retina. © REM 2005.

The description of human retinal neuron distributions and patternings in Oyster<sup>1</sup> is without peer and will only be summarized briefly. The relative numbers of rods and cones change radically across human retina (Fig. 12.19), ranging from

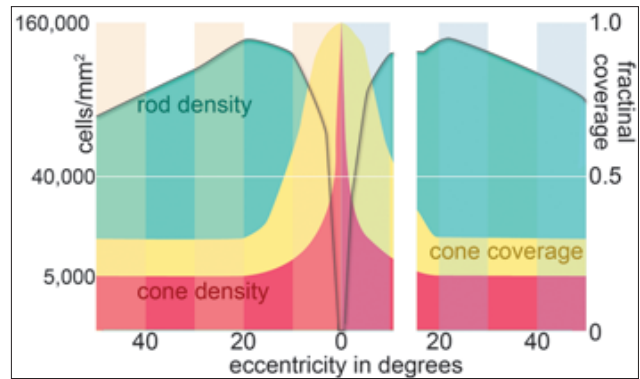


**FIGURE 12.19.** Sampling of image space by photoreceptors. Cone density (red), rod density (cyan), and cone coverage (yellow) profiles in the human retina as a function of retinal eccentricity in the equatorial plane. Temporal retina is left and nasal is right on the abscissa, with a gap centered on ~14° eccentricity representing the optic nerve head. The left ordinate is density data replotted from Curcio<sup>129</sup> on a square root scale. The right ordinate is linear fractional coverage: the fraction of image space captured by cones. Cone density forms a wide pedestal at ~5000 cones/mm<sup>2</sup> with an extremely steep peak in the central 2° reaching ~160 000 cones/mm<sup>2</sup> in the foveola. Rod density is a broad profile of 90 000–140 000 rods/mm<sup>2</sup> that would also peak at ~160 000 rods/mm<sup>2</sup> were it not for a deep declivity formed by their displacement in the central 2°. The foveola is rod free. Cone myoid and ellipsoid diameters increase with eccentricity so that cones never capture less than ~30% of the available image data.

~160 000 cones/mm<sup>2</sup> at the foveola to 5000 cones/mm<sup>2</sup> at ~20° eccentricity.<sup>1,129</sup> Rods show a broad profile ranging from ~90 000 to 140 000 rods/mm<sup>2</sup> with shoulders at ~15–20°. But it is clear from the trend that rods would also peak in the central retina at ~160 000 rods/mm<sup>2</sup> were it not for the fact that cones displace them. This is about the maximum density possible for any photoreceptor, corresponding to a spacing of ~2.5 μm (including MC space at the ELM). As cones develop early and capture the foveola, rods can encroach only from the outer margins, leading to a deep declivity in the rod profile and a rod-free foveola. In addition to changing density, cone size also changes with eccentricity. While this negatively affects acuity, it increases cone photon capture. In fact, the coverage factor (CF) of the cone mosaic (the fraction of the retinal image captured by cones) never drops much below 0.3 outside 15°, and smoothly rises to 100% over the foveola. Remarkably, overall cone density in rodents<sup>130</sup> can be much higher than primate peripheral cone density, reaching ~12 000 cones/mm<sup>2</sup>. But as rodent cones and rods are similar in size and cones comprise only 3% of the photoreceptors, their coverage is only 0.03. The significance of this is more obvious when we normalize sampling for the relative optical sizes of the eyes (Table 12.2.4). An image in peripheral human retina that subtends a circle 1° in diameter covers a patch of 425 cones, whereas the same 1° image in mouse<sup>131</sup> covers a patch of only eight cones. The statistical danger of generalizing visual losses or recoveries in mouse models of retinal degeneration should be gauged carefully.<sup>11</sup>

Relative acuity loss with eccentricity in the human eye is partially a consequence of cone density decline and partly the increased receptive field sizes of retinal GCs that drive perception. Indeed, many neuron classes show large changes in local density over the eye.<sup>1</sup> The foveola itself (the central 20 s arc of the retina) is composed solely of cones with all other neurons and cone axons and pedicles displaced to a ring around the foveola. However, the corresponding GC and BC density

## RETINA AND VITREOUS

profiles roughly track cone density. The cortical magnification factor (the disproportionate area of cortex devoted to foveal vision), reflects a relatively constant volume of cortex captured per GC axon. Visual acuity doesn't simply follow either cone density or the density of midget GCs. A mixture of GC sampling units exists at any retinal position. GCs with small receptive fields they can resolve smaller targets, but not as light sensitive as those with larger receptive fields. Thus supra-threshold acuity depends highly on image contrast and mean luminance. Multiple classes of sampling units likely participate in setting visual performance.

Large-scale chromatic patterning also accompanies these variations in cone density. Many species show variations in the distributions of blue cones, with many mammals (some rodents and lagomorphs), exhibiting ventral (inferior) fields entirely composed of or enriched in blue cones.<sup>132-134</sup> No exploration has been made of connectivity in these regions, but one might imagine that BCs or HCs that might avoid blue cones elsewhere cannot do so in these regions; or they may be excluded from them. Blue cones are not the only variable types. The linear visual streak in turtles, where cone densities approach primate foveal levels, is disproportionately enriched in red cones expressing VP620 and red oil droplets. The temporal foveas of some avians are positioned within a red-field some 4–5 mm in diameter highly enriched in red cones expressing VP580 and red oil droplets. Finally, but no less compelling, the tritanopic or blue-blind fovea of the primate foveola is a small zone of ~15 min of arc with few or no blue cones.<sup>24,135,136</sup> Roughly following rods, blue cones increase in frequency until they represent 5–10% of the cones (depending on species), peaking at ~0.3–1°, thereafter following the density decline of the cones. The mechanisms controlling fine these variations are unknown but the molecular control of overall cone differentiation may involve selective fibroblast growth factor (FGF) receptor expression.<sup>137</sup> The mechanism that prevents mature blue cone expression in the foveola also may regulate patterning of the rods.

### FINE-SCALE PATTERNING OF RETINAL CELLS

The retina is an assembly of sampling units that cover the image plane.<sup>1</sup> Over 60 classes of neural elements are patterned across this plane and, if we treat them as tiles, we find them arranged in different pattern types,<sup>1,138</sup> partly quantified by their CFs.

- Packings have no overlaps: Photoreceptor arrays are packings with  $CF < 1$
- Coverings have no gaps: AC arrays are coverings with  $CF > 1$
- Tilings have no overlaps or gaps: BC and GC arrays resemble tilings with  $CF \sim 1$
- Mosaics are general patterns of any type, with tile subtypes.

Cone arrays are mosaics of three tile subtypes [R, G, B] with  $CFs < 1$  (Fig. 122.20).  $CFs$  for complex, branched cells such as HCs, ACs, or GCs can be more precisely defined as  $CF = A \times D$ , where  $A$  is the dendritic or receptive field area (defined as its convex hull or Voronoi domain) of a single cell in a given class and  $D$  is the density of cells per unit retinal area. Thus, an AC with a dendritic field 0.5 mm in diameter and a density of 200 cells/mm<sup>2</sup> has a  $CF$  of 39; each point in the image is sampled by the receptive fields of 39 ACs of that class. Each kind of retinal neuron has a coverage that reflects the sampling necessary to create a seamless set of signals. Patterns can be very orderly (crystalline), statistically orderly, uniformly disorderedly (random) or statistically clumped. One measure of order within a cell class is the conformity ratio:  $CR = NND/s$ , where  $NND$  is the mean nearest-neighbor spacing between cells in a class and  $s$  is the standard deviation of that spacing.<sup>139,140</sup> For large samples,  $CR \sim 3$  when patterns are statistically orderly and  $C > 10$  when patterns become nearly crystalline, with clear axes of object orientation. The primate peripheral blue cone pattern can reach  $CR > 3-5$ , while patterning near the fovea seems random. Human blue cone patterns seem less rigid than those of other primates. Nonmammalians, especially teleost fishes, can display stunning crystalline mosaics<sup>141</sup> and blue cones in those mosaics have  $CR$  values approaching 30 (Fig. 122.18), which is so precise that such images can be used as optical diffraction masks. No mammalian neuron has patterning this rigid. Conversely, widely spaced cells such as dopamine neurons, other AxCs and IPCs<sup>142</sup> in many species have apparently random mosaics. This would be expected of neurons with global signaling modes, mediated more by volume diffusion (e.g., dopamine) than by specific cell contacts. Again,  $CR$  is of more than academic interest. Though the genetic and signaling mechanisms that control spatial patterning are still largely unknown,<sup>143,144</sup> defects in these pathways may cause serious sensory impairment.

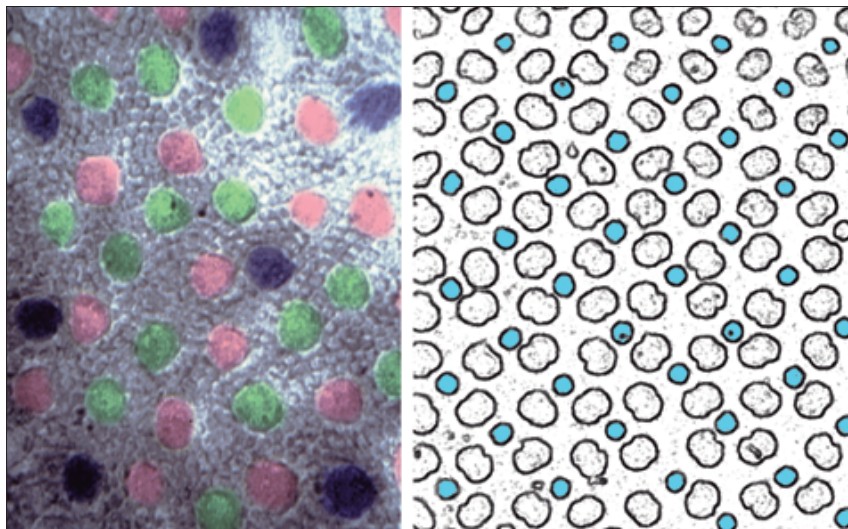


**FIGURE 122.20.** Fine-scale cone patterns. (Left) Blue cones in the baboon retina visualized with a redox probe (135). The nonblue cones were randomly selected to represent VP560 (red) or VP530 (green) cones. The blue cone  $CR$  is 5.5 in the larger data set (not shown). (Right) Precise blue cone patterns from flatfish retina (*Pleuronectes* sp) associated with a precise, repeating cone mosaic, with  $CR = 26.7$ . (Left) © REM 2003. (Right) Derived from Engstrom K, Ahlbert IB: Cone types and cone arrangement in the retina of some flatfishes. *Acta Zool* 1963; 44:1–11, edge filtered and thresholded.

AU:  
Is 135 the  
reference  
number?

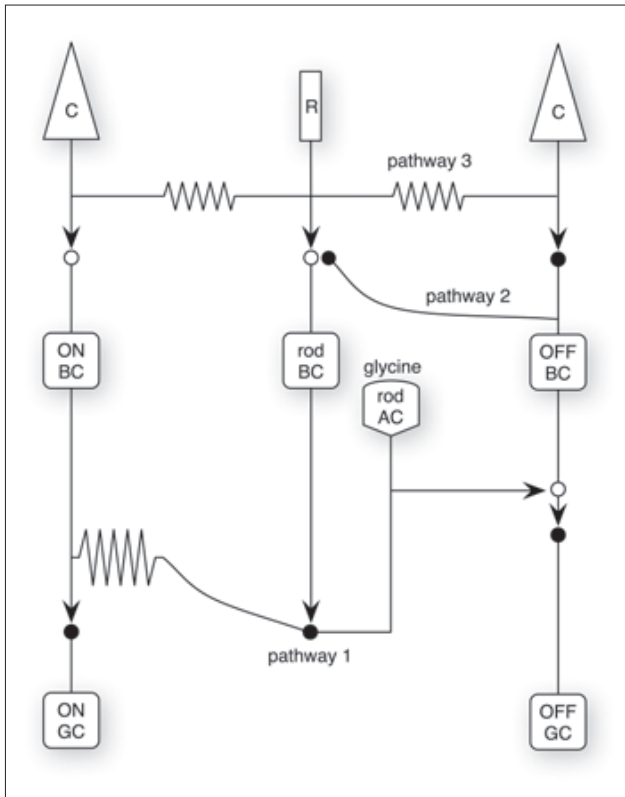


**FIGURE 122.21.** Three major rod pathways in the mammalian retina. Pathway one is initiated by the high-gain rod  $>$  rod BC  $>$  glycinergic rod AC chain. Glycinergic rod ACs are fanout devices that pass rod signals to ON cone BCs via gap junctions (resistor symbol) and to OFF cone BCs via sign-inverting glycinergic synapses. Pathway 2 is initiated at higher scotopic brightnesses by direct rod  $>$  OFF BC signaling. Pathway 3 is initiated by small gap junctions (Fig. 122.8) at mesopic ranges and mediate signaling directly through cone pedicles. © REM 2005.

## THE BASIC PATHWAYS OF RETINAL SIGNALING

### The Basic Rod Pathways

Five discrete variants of three major pathways inject rod signals into the visual system (Fig. 122.21, Box 122.7).<sup>18</sup> No known GC population exclusively carries rod signals, although it was reported that GC-like bipelexiform cells made direct rod contacts with their dendrites.<sup>145</sup> This CG has not yet been validated to form a distinct population in the mammalian retina. In pathway 1, the so-called 'starlight' circuit, narrow-field glycinergic rod (AII) ACs collect signals from several rod BCs and redistribute them via gap junctions to ON cone BCs and via sign-inverting glycinergic synapses to OFF cone BCs. The same brain pathways that carry cone signals process perception of scotopic signals. At near-threshold levels, detection is mediated

### BOX 122.7 Multiple pathways for rod signals

- Canonical "Starlight" pathways
  - Canonical Scotopic OFF pathway  
rods  $>$  rod BCs  $>$  rod ACs  $>$  OFF cone BCs  $>$  OFF cone GCs
  - Canonical Scotopic ON pathway  
rods  $>$  rod BCs  $>$  rod ACs  $>$  ON cone BCs  $>$  ON cone GCs
- Noncanonical "Moonlight" pathway
  - Noncanonical direct OFF pathway  
rods  $>$  mixed OFF BC  $>$  OFF cone GCs
- Noncanonical "Twilight" pathways
  - Noncanonical OFF coupling pathway  
rods  $>$  cones  $>$  OFF cone BCs  $>$  OFF cone GCs
  - Noncanonical ON coupling pathway  
rods  $>$  cones  $>$  ON cone BCs  $>$  ON cone GCs

by these high-gain canonical scotopic ON and OFF pathways. The integration of rod signals by rod BCs generates a response far more sensitive than an individual rod.<sup>18</sup> Rod BCs drive glycinergic rod ACs with AMPA receptors, making the glycinergic rod AC one of the most light-sensitive elements in the retina.<sup>146</sup> Glycinergic rod ACs, or perhaps the aggregate IPL rod network, likely generate the scotopic threshold potential of the ERG.<sup>147</sup> At slightly higher brightnesses, it is thought that a small population of OFF cone BCs behave as mixed rod-cone BCs (a cell type abundant in nonmammals<sup>19</sup>) and collect a small number of rod inputs.<sup>18</sup> These cells may require higher brightnesses and larger rod responses to generate perceptual responses. Why these are segregated to OFF channels remains unclear, and these paths have only been found in nonprimates so far. However, Li et al.<sup>148</sup> have shown that all rabbit OFF BC classes show some minor rod input, though not all individual cells do. Any cell in the equivalent of class dB2 and dB3 BCs has ~80% chance of contacting a few rods. Finally, in the mesopic range where both rods and cones begin to operate, a 'twilight' system allows significant leakage of numerous rod signals into a sparse array of cone pedicles directly.

### The Achromatic Cone Pathways

As normal human vision seems richly colored, the concept of abundant achromatic channels seems odd. But sampling units in retina must measure the spectral dispersion of light reflected from an object as the sum of R+G+B (or at least R+G) signals so that the visual system can encode both object brightness and the spectral purity or saturation of a patch of light. This is one role of the diffuse cone BC system. Put simply, these cells collect summed cone signals and pass them on to parasol GCs and other wide-field GCs (Fig. 122.22, Box 122.8). However, the pathways for brightness are clearly more complex, as color-coded midget systems become noncolor-coded in parafovea and beyond, as they randomly collect signals from midget BCs

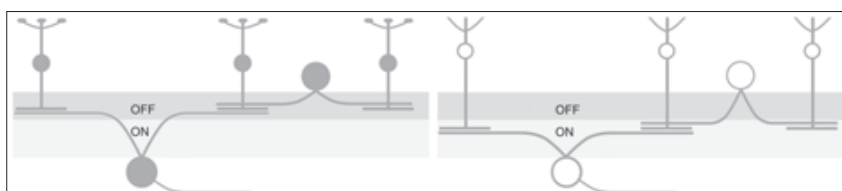


**FIGURE 122.22.** Wide-field achromatic signaling via OFF (left) and ON (right) parasol GCs in primate retina. Each GC collects signals directly from a set of diffuse cone BCs in its central dendritic field and captures sign-inverting signals from distant BCs via BC  $>$  AC  $>$  BC  $>$  GC lateral feedback and BC  $>$  AC  $>$  GC lateral feedforward chains. © REM 2005.

AU: Please provide expansion of ERG.

AU: Please provide expansion of ERG.



## RETINA AND VITREOUS

**BOX 122.8 Pathways for diffuse cone BC signals**

- Major Diffuse OFF pathways
  - cones > diffuse OFF KA BCs (dB1, dB3) > OFF cone GCs
  - cones > diffuse OFF AMPA BCs (dB2) > OFF cone GCs
- Minor Diffuse OFF pathways
  - rods > diffuse OFF BC (mostly dB2, dB3) > OFF cone GCs
- Diffuse ON pathways
  - cones > diffuse ON BCs (dB4, 5, 6) > ON cone GC

**BOX 122.9 Pathways for blue cone signals**

- B+ center/Y- center pathway:
  - B cones > blue ON BCs > B+/Y- small and large bistratified GCs
  - RG cones > diffuse OFF KA BCs (dB2) > B+/Y- small and large bistratified GCs
- Blue OFF center/surround pathways
  - B cones > blue OFF midget BCs > blue OFF midget GC
- B-/Y+ large field pathways
  - Pathway for B cones not known for this cell

contacting R and G cones.<sup>108</sup> There are two likely pathways for cone OFF BCs. Extending concepts gleaned from homologous BCs in ground squirrel retinas, primate class dB1 and dB2 likely use KA receptors,<sup>64–65</sup> which are highly glutamate sensitive, explaining the positioning of their dendrites as flat contacts far from the ribbon active site. KA receptors are also slightly slower and more sustained in current responses than AMPA receptors likely used by dB3 cells. The idea that AMPA and KA receptors parse the visual world into more and less transient temporal events deserves careful analysis. Consistent with this, it would appear that large transient GCs sample from the from dB3 arbor.<sup>79</sup>

**The Blue Cone Pathways**

Blue ON / yellow OFF (B+/Y-) GCs are the only known mammalian retinal cells with spectrally biphasic receptive field centers.<sup>82,108</sup> Many nonmammals have such color-opponent GCs, BCs, and HCs.<sup>101</sup> Both large and small classes of bistratified GC sample from level 80 of the IPL to capture signals from the unique blue cone BCs and levels 20–30 to capture dB2 BC R+G signals (Fig. 122.23, Box 122.9).<sup>69</sup> It is presumed that both arbors of the B+/Y- GCs express the same

mixture of AMPA and NMDA receptors, but this is not known. Recent evidence suggests the existence of a midget blue-OFF pathway,<sup>61</sup> although how this cell would function in vision is less clear given the problem of chromatic aberration, where optimal focus on R and G cones would blur images on the B cone mosaic. Blurring is arguably one of the selection pressures forcing sparse distributions of B cones in all species. Finally, the newly described melanopsin GC is a large-field Y+/B- cell,<sup>83</sup> though the path by which the B- signals are acquired is not clear.

**Red-Green Color-Opponent Pathways**

Since the early 1970s it has been clear that the primate retina passes an assortment of color opponent signals to the LGN and that these tend to be grouped into four categories:

- R+ center / G- surround
- R- center / G+ surround
- G+ center / R- surround
- G- center / R+ surround.

One physiological view originally held that the surround paths of midgets must also be spectrally pure, while other studies support spectral mixing by random contacts.<sup>73,108,149–151</sup> On balance, the evidence suggests that cone-specific contacts are not present in the R and G channels of the primate retina. For example, though a midget BC → midget GC transfer may report the signals of a single R cone, the ACs that comprise the lateral elements collect from nearly all adjacent midget BCs,<sup>152</sup> so that the composition of the surround might be spectrally mixed (Fig. 122.23, Box 122.10). And if HCs clearly collect from all cones or at least R+G cones, that mixture might be present in all midget BC surrounds.<sup>153</sup> If R and G cones are not chromatotypes and downstream BCs, ACs, and GCs make opportunistic contacts, how can nearly pure R or G surrounds

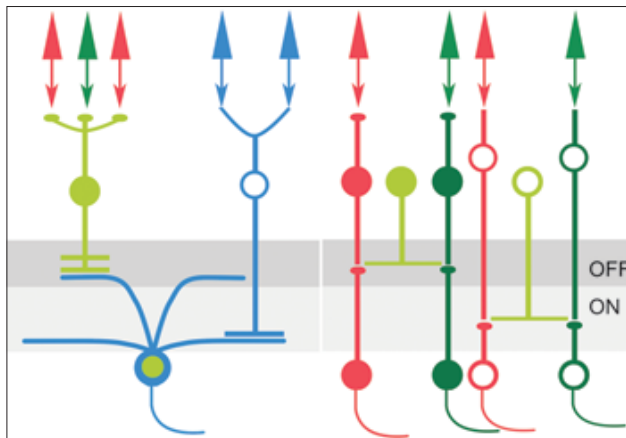


**FIGURE 122.23.** Narrow-field chromatic signaling in bistratified blue ON/yellow OFF GCs (left) and monostратified ON and OFF foveal midget (right) GCs in primate retina. Blue ON signals are captured via blue cone > blue BC > blue GC chains in the proximal arbor. Yellow (R+G) OFF signals are captured via R + G cone > dB2 OFF BC > blue GC chains. Midget GCs that contact single cones have pure R (VP560) or pure G (VP530) centers and AC-mediated surrounds driven by varied mixtures of R+G cones. There is also evidence for blue cone > OFF midget BC signaling (not shown).  
© REM 2005.

**BOX 122.10 Pathways for red and green cone signals**

- Red or Green ON center pathway:
  - R or G cones > midget ON BC > midget ON GC
- Red or Green ON center pathway:
  - R or G cones > midget OFF BC > midget OFF GC
- Generic surround pathways:
  - RG cones > H1 HC > RG cones > ...
  - RG cones > H1 HC > midget ON BC ...
  - RG cones > H1 HC > midget OFF BC ...
  - R and G midget BCs > small-field ACs > midget BCs > midget GC
  - R and G midget BCs > small-field ACs > midget GC



**BOX 122.11 Increment spectral sensitivity functions in trichromatic primates**

- The absorption peaks of cones do not predict the daylight increment threshold spectral sensitivities of primates (Fig. 122.24).
- No sum of absorptions reproduces the spectral sensitivity envelope.
- Cones express VP560 (yellow-green), VP530 (green), or VP420 (violet-blue).
- Sensitivity peaks are 610 nm (orange-red), 520–530 nm (green), and 430 nm (blue).
- A number of factors shape the sensitivity channels of the eye, but the most important are opponent interactions.
- In the absence of opponent functions, the R sensitivity peak moves to the VP peak:  
If green cones are desensitized by adapting lights, the long-wave sensitivity peak progressively moves from 610 to 560 nm.

appear?<sup>149</sup> The answer may partly come from two features of cone patterning. First, the proportions of R and G cones can vary across individuals (and perhaps species), with human R:G values ranging from 16 to 1.<sup>154–156</sup> Second, fine-scale patterning of R and G cones is often statistically clustered rather than randomly uniform.<sup>156</sup> Thus a single G cone → midget BC → midget GC chain in an R cone-dominated retina may show nearly pure R surround signaling. And similarly, that chain in a retina with equal numbers of R and G cones can plausibly be found centered in a patch of R cones, since the dendritic fields of ACs associated with midget cells also tend to be small.<sup>157</sup>

Given the individual variability in the R/G cone ratio, it is surprising that many aspects of color vision seem stable across individuals, such as the photopic increment threshold spectral sensitivity (see Box 122.11, Fig. 122.24) and the wavelength of unique yellow.<sup>158</sup> Other measures that probe the densities of current generators in the eye (e.g., the ERG spectral sensitivity) show that known variations in the R/G ratio roughly predict spectral peaks.<sup>158</sup> Perception does not vary much. This suggests that there is a normalization mechanism in the visual system, such as activity-dependent axon sorting; a major mechanism for organizing sensory fields. Cortical area V2 in macaque shows strong evidence of such spectral sorting.<sup>159</sup> Furthermore, color perception itself shows evidence of highly plastic properties that tune vision, perhaps regardless of R/G cone ratio.<sup>160</sup>

**Melanopsin Pathways**

The melanopsin pathway is an exciting discovery, but not easy to understand as these cells integrate signals from rods, cones and their own intrinsic phototransduction. Dacey et al show that primate melanopsin GCs are also rare Y+/- cells but that both inner and outer classes of melanopsin GCs show the same polarity of response.<sup>83</sup> The signaling channels for melanopsin GCs (Box 122.12) include rods and cones via directly glutamatergic AMPA and/or NMDA receptors. The intrinsic 11-cis retinaldehyde isomerization coupled transduction<sup>88</sup> accesses an unknown conductance to initiate spiking. Melanopsin GCs appear to be a diverse population morphologically and target the LGN, SCN, and olivary pretectum. The fact that they project to LGN and give extremely sustained light responses proportional to flux over many decades<sup>83</sup> argues that they may correspond to intrinsic luminosity cells of the visual system.

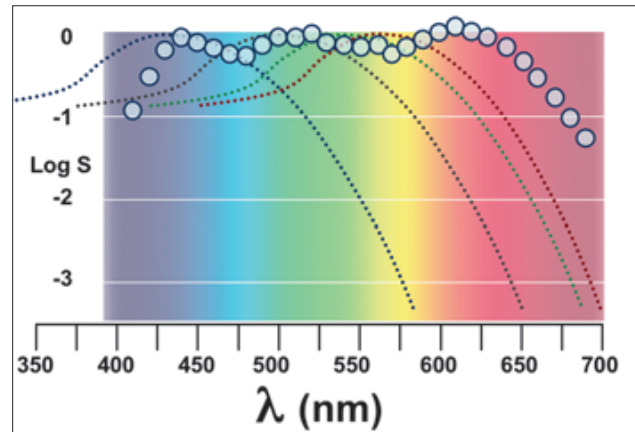


**FIGURE 122.24.** The mismatch between primate photopic spectral sensitivity profiles and VP absorption functions plotted on a normalized  $\log_{10}$  sensitivity ordinate ( $\log S$ ) and a linear wavelength abscissa ( $\lambda$ ). Dotted lines from left to right are normalized VP420, VP499, VP530, and VP560 absorbance functions. The circles are the 4-day mean increment threshold spectral sensitivity for a rhesus monkey in  $\log S = \log (1/Q)$  for a  $2^\circ$  foveally centered test flash on a  $10^\circ$  neutral white 10 000 K background Maxwellian view field. Data recorded by REM in 1971. There are several mismatches with the pigment curves: (1) The long- $\lambda$  peak is at 610 nm; (2) The mid- $\lambda$  complex is broad; (3) There is a minimum at 580 nm; (4) There is a minimum at 470 nm; (5) The short- $\lambda$  peak is at 450+ nm; (6) The short- $\lambda$  band is narrow; (7) No sum of VPs matches the spectral sensitivity. © REM 2005.

**BOX 122.12 Speculative pathways for melanopsin GCs**

- RG Cones > i ON diffuse BCs (dB6?) > inner melanopsin GCs
- RG cones > OFF diffuse KA BCs (dB1?) > GABA ACs > i outer melanopsin GCs
- B cones > i blue ON BCs > GABA ACs > i inner melanopsin GCs
- B cones > ? > outer melanopsin GCs
- Melanopsin GCs > LGN > Cx > brightness perception?
- Melanopsin GCs > SCN > photoentrainment
- Melanopsin GCs > pretectum > pupillary reflex

AU:  
What does  
'?' stand for  
in boxes.  
Please  
check.

**FURTHER ELEMENTS OF RETINAL STRUCTURE****INTRODUCTION**

The retina is a complex, dynamic neural structure. Despite the accumulation of apparently precise pathway models, they are incomplete in many ways. The modes and weights of HC signaling are still uncertain. The most common synapses in the IPL, serial AC → AC elements, have had no formal place in any model until recently. Many modes of physiological signaling involve widespread targets and multiple sources, including retinal efferents, and their roles in vision is not understood. MCs could clearly locally modulate neural efficacy through ATP-gated channels and regulation of extracellular ion and neurotransmitter levels, but it is not known if they do. Visual experience in development influences GC maturation and loss of visual drive in retinal degenerations triggers neural

## RETINA AND VITREOUS

remodeling of the retina. Some GCs are intrinsically photosensitive, as has been seen. This next section will briefly review the imports of some of these topics.

### SERIAL SYNAPSES AND NESTED FEEDBACK

Serial AC  $\rightarrow$  AC synapses comprise about two-third of the IPL synapses in nonmammals<sup>161</sup> and a smaller fraction in mammals,<sup>162</sup> yet they had no established role in any pathway, until recently. Indeed, AC  $\rightarrow$  AC  $\rightarrow$  AC triplets are far from rare, which offers significant opportunities to shape circuits, but why? And how? At the least, this argues that most network models are incomplete. Some evidence indicates that such synapses are part of nested feedback and feedforward paths

- Feedback: BC > AC > i BC
- Nested Feedback: BC > AC > i > AC > i BC
- Feedforward: BC > AC > i GC
- Nested Feedforward: BC > AC > i > AC > i GC

Concatenating sign-inverting paths formally represent positive feedback, which is potentially destabilizing: AC > i AC > i BC  $\equiv$  AC > BC. Biological reality is more complex. First, the abundance of serial chains means that positive feedback, if it occurs, does not destabilize vision. Second, these signals are progressively delayed in time, so their effects do not sum statically. Finally, the gains of inhibitory synapses are typically fractional (<1), so the net pathway gain becomes even smaller.<sup>161</sup> This suggests that serial synapses could effectively shape many pathways in subtle ways and may be generic to many feedback and feedforward networks.

More recently, Hennig et al<sup>163</sup> implemented nested AC elements in a comprehensive mathematical model of linear and nonlinear retinal GC signaling, and found that the influence of nesting was weak, consistent with subtle shaping rather than destabilizing positive feedback. Results from the laboratory of the late Ramon Dacheux strongly implicate serial synapses in signaling asymmetries that may contribute to the directional biases of DS GCs.<sup>80,164</sup>

### EFFERENTS

Efferent pathways from CNS systems are well known in nonmammals but have been controversial in mammals, though both Ramón y Cajal<sup>165</sup> and Polyak<sup>166</sup> described them. Polyak clearly identified efferent fibers in the optic nerve that arborized in the IPL of primate retina<sup>166</sup> and separate serotonin- and histamine-immunoreactive efferents targeted the IPL have now been described.<sup>167-170</sup> The roles of these efferents for vision remains unknown, but the close association of both systems with retinal vessels is provocative. Further, both rod and cone ON BCs in baboon express HR3 histamine receptors on their dendritic tips, but the relation between neuronal expression of histamine receptors and IPL efferents is uncertain.<sup>171</sup> However, the discovery of serotonin-immunoreactive efferents gives the first compelling physiological drive path for serotonin-receptor systems in the retina, as there are no known intrinsic serotonergic neurons in the mammalian retina, unlike nonmammals<sup>3</sup> which express elegant wide-field GABAergic/serotonergic ACs.

### THE DOPAMINE PATHWAY

Dopamine neurons represent the quintessential AxC pathway.<sup>3,18,171</sup> The dominant TH1 (tyrosine hydroxylase type 1) AxCs, are narrowly stratified cells that arborize at level 0-10 of the IPL with medium-field dendritic arbors and fine, complex axon terminal fields.<sup>172</sup> It has long been suspected that

most retinas harbor more than one class of TH immunoreactive cell<sup>173,174</sup> and rodents clearly possess at least two; TH1 cells are typical AxCs and are not GABA immunoreactive, while TH2 cells are more AC-like (lacking axons), often express epitope-masked or phosphorylation-masked TH immunoreactivity and are also GABA immunoreactive.<sup>175,176</sup> TH1 AxCs appear to be spontaneously spiking 'clock-like' cells that resemble spontaneously signaling dopamine neurons in brain.<sup>177,178</sup> They have some weak excitatory inputs but many inhibitory inputs and appear to be under strong GABAergic control.<sup>3</sup> In any case, TH1 cells appear to be activated by photopic stimuli, making them signalers of dawn. Dopamine released by vesicular means probably diffuses through the retina to its various targets.<sup>171</sup> Virtually every class of retinal cell, including photoreceptors and MCs has been reported to express dopamine receptors.<sup>171</sup> Basically, dopamine signals appear to light-adapt the retina by diverse G-protein coupled mechanisms such as HC uncoupling<sup>179</sup> and enhancement of GC response speed.<sup>180</sup> The scale and scope of these adaptive signals are under intense study, but it is of great interest that retinal dopamine cells also display high levels of circadian clock gene expression, potentially making them key elements for intrinsic retinal photoperiod control.<sup>181</sup> This pathway appears separate from the melanopsin GC path, but it is intriguing that the dendrites of outer melanopsin GCs co-stratify with TH1 cells.

### NONCANONICAL SIGNALING MODES

In many ways the retina is a complex neuroendocrine organ whose operations we understand poorly. We can only offer brief survey of many intrinsic 'parahormonal' systems in retina that depend on nonvesicular or diffusion-based signaling (e.g., dopamine neurons). Photoreceptors are known to synthesize and release melatonin at night, and this signaling is thought to modulate both RPE-mediated photoreceptor outer segment phagocytosis and the activity of dopaminergic neurons.<sup>3,182</sup> There is now evidence, in addition to cyclic constitutive regulation, that excessive melatonin exposure enhances the sensitivity of photoreceptors to light damage and specifically regulates the expression of a restricted set of ocular genes.<sup>182</sup>

Neurons with the capacity to express high levels of nitric oxide (NO) synthase and generate NO as a signaling molecule have been termed *nitrergic*.<sup>3,8,183</sup> Some of these cells are clearly AxCs.<sup>8</sup> By local diffusion across cell membranes, NO binds to the heme core of soluble guanyl cyclase and activates high levels of cGMP production which, in turn, has the capacity to modulate gap junction permeability<sup>184</sup> as well as open local cyclic nucleotide gated cation channels. The regulation of these systems and their light stimulus selectivities are not well known and it is suspected that many cell classes can produce NO beyond the identified nitrergic AxCs.<sup>183</sup>

GABA has intermittently been identified in BCs of the mammalian retina, including cat and monkey, with no clear mechanism of action (3). Recently it has been suggested that a set of OFF cone BCs in cat retina similar to dB1 in monkey are dual GABA/glutamate-releasing neurons.<sup>185</sup> The co-stratification of the terminals of these BCs with the dopaminergic TH1 plexus in the distal IPL suggests the possibility of OFF BC > i dopamine AC signaling, which would be consistent with the apparent depolarization of dopamine cells by light, yet restriction of synaptic inputs to the OFF BC region of the IPL. GABA-immunoreactive BCs appear more abundant in monkey and it is not clear, however, that they can all be OFF BCs.

MCs and the optic fiber layer are key positions to modulate the signaling of neurons in the retina. Indeed it appears that excitation-induced calcium waves that propagate locally in the GCL and OFL in the astrocyte and MC network can directly

modulate GC excitability.<sup>186</sup> Moreover, MCs have now been shown to release ATP, which may directly activate calcium entry via purinergic receptors on vascular pericytes, in turn triggering local vasoconstriction.<sup>187</sup> Thus retinal activity has the potential to locally regulate blood flow through MC signal integration. The scope and strength of such MC signaling is yet unknown.

Peptide-releasing neurons in the mammalian retina include different cohorts of wide-field GABAergic ACs that express neuropeptide Y (NPY), substance P (SP) or vasoactive intestinal peptide (VIP), AxC-like cells expressing somatostatin (SRIF) and minor (but not necessarily unimportant) populations expressing several other neuroactive peptides.<sup>37</sup> The detailed relationships between fast neurotransmitter versus slow peptide secretion signaling from the same cell are simply unclear. But it has long been suspected that peptide-containing vesicles are released by an exocytosis mechanism that requires much more calcium entry (and hence stronger depolarization) than fast neurotransmitter vesicle fusion. Even when there is evidence of a possible signaling mode, we have little insight as to the purpose. For example, SRIF appears excitatory on a seconds-to-minutes timescale in GCs<sup>188</sup> and induces an increase in input resistance in ON BCs.<sup>189</sup> How these events are related remain unclear. Though it is widely accepted that specific peptides likely have circuit-specific modulatory functions, specific roles in any of the canonical pathways are not known. It is also not known how far peptides diffuse and how long they persist in the extracellular space. Other peptide-like associations have even less certain functions. The blue cone BCs of primates also express cholecystokinin (CCK)-like immunoreactivity<sup>26,37</sup> and CCK does suppress GC activity, but no correspondence has been established for this in the canonical blue cone → blue cone BC → B+/Y- GC pathway. And it is not clear that blue cone BCs actually release bona fide CCK.

### ACTIVITY-DEPENDENT PLASTICITY, RETINAL REMODELING, AND PHOTORECEPTOR DEGENERATIONS

The elegant structure of the mammalian retina can no longer be viewed as static and hard-wired. Indeed, the retina undergoes postnatal refinement in synaptic connectivity,<sup>190,191</sup> possible revisions in gene expression in response to visual environments at maturity, and reactive rewiring when challenged by photoreceptor degenerations.<sup>11</sup> We are only beginning to understand the scope of these physical transformations, but it is now clear that adult retinal neurons can revise their patterns of synaptic contacts and generate new processes.<sup>11</sup> During postnatal life in rodents, the visual environment influences the onset of bouts of spontaneous signaling thought to be required for synaptic maturation<sup>144,190</sup> and modulates the segregation of the IPL into ON and OFF sublayers, apparently through a dendritic pruning process.<sup>191</sup> While previous research in the 1970s produced contentious views on activity-dependent retinal maturation,<sup>11</sup> many studies can now be revisited in light of modern findings. The IPL is clearly the site of most of these effects, but it would now be imprudent to exclude the OPL.

Recently, Fisher and colleagues have detailed a range of cellular remodeling phenomena and mechanisms including rapid neurite sprouting, neuronal migration and MC hypertrophy in response to chronic retinal detachment.<sup>192</sup> These plastic abilities of adult neuron cells presaged discoveries perhaps even more surprising to retinal biologists (but not to CNS biologists); the amazing propensity for retinal neurons to rewire aggressively in response to retinal degenerations.<sup>11,193</sup> So far, all known photoreceptor degenerations trigger major revisions of retinal circuitry in three phases.<sup>11</sup> In phase 1, photoreceptor stress triggers the retraction of BC dendrites from

rod and or cone synapses. Indeed, the first signs of visual impairment in RP are likely to be a result of the phase 1 loss of dendritic compartment in BCs before there is significant loss in photoreceptor signaling. Indeed, given the ability of BCs to report even small photoreceptor signals, early visual impairment more readily implies defects in synaptic signaling than phototransduction. The diverse genetic types of RP exhibit different modes of photoreceptor loss. If the mode of degeneration is cone-sparing, rod BCs attempt to transiently capture inputs from surviving cones. If the degeneration is rod-cone lethal, all BCs disassemble their dendritic modules, including their signaling receptors. In phase 2, photoreceptor death leads to loss of the ONL and the development of a MC seal between the remnant RPE (if it survives) or the choroid and the remnant neural retina. Finally, in phase 3, the retina undergoes a prolonged epoch of revision that involves additional neuronal death, formation of new process fascicles and new ectopic synaptic microneuromas, and even neuronal migration leading to mixing of the INL and GCL through disrupted zones of the IPL.<sup>11,193</sup> Synaptogenesis leads to new networks in microneuromas, and these networks appear to be random collections of opportunistic connections. These generate networks that seem optimized for self-excitation rather than visual signaling.<sup>194</sup> In general, these transformations challenge therapeutic intervention windows and repair strategies of all types, from genetic to bionic, for all forms of retinal degeneration.

### SUMMARY AND PERSISTENT QUESTIONS

Our understanding of the populations of neurons that make up a retina has expanded. Clearly, at least 60 and maybe even 80 cell classes are involved, and our catalog is likely to become even more detailed.<sup>195</sup> Though most of the canonical pathway neurons have likely been identified, every pathway is beset with questions regarding signaling modes and strengths; almost every pathway has undefined synaptic partners, especially among the AC cohort; and every retina almost certainly harbors small populations of poorly defined or even yet-unknown neuron classes.<sup>195</sup> Sparseness or difficulty in identification of a cell class does not imply relative unimportance. TH1 dopamine AxCs are among the rarest of neurons in the ACL and their actions are global and powerful. Melanopsin GCs are among the rarest of GCs and they are essential carriers of photoperiod and pupillary control signals. We still do not have a proven role for a clearly heterogeneous set of retinal efferent fibers originating in hypothalamus and brainstem.

Even simple issues, such as how neurons choose partners to contact, remains elusive. This is especially true of the R and G cones of trichromatic primates, which seemed to have evolved so recently via VP gene duplication that no other gene expression differences have clearly emerged that would 'label' them as specific chromatotypes for putative R-G opponent neurons, as did occur in nonmammals. Conversely, B cones and rods each express many different genes (beyond VP expression), some of which clearly drive formation of selective contacts. But what are we to make of new patterns of cones that selectively express vGlut2 but are still G cones in mouse,<sup>29</sup> or sparse human cones that express no opsin except melanopsin<sup>30</sup>?

HCs, the first cells in the outer retina from which intracellular recordings were ever made, remain one of the most enigmatic. Are they truly neurons? How do they signal their targets? Why do they form nearly half of the capillary endothelial ensheathment in the mature retina?<sup>196</sup> What does the rod-specific axon terminal actually do? Is signaling transmitter-mediated by GABA or is it ephaptic, or both? Why do most HCs express no GABA? Where are the vesicles and are the vesicles we can see presynaptic or cargo vesicles?



## RETINA AND VITREOUS

What are the selective roles of H1 and H2 HCs. And where is the H3 HC array?

The BC population is clearly settling into 10 defined classes; a single rod BC class, a single blue cone ON BC class, two midget cone BC classes (ON and OFF), and at least three classes each of diffuse ON cone BCs and diffuse OFF cone BCs. The canonical rod → rod BC → rod AC → cone BC → cone GC pathway has now been augmented with a minor rod → diffuse OFF cone BC → OFF cone GC path, owing to very small numbers of rod contacts made by some OFF cone BCs.<sup>148</sup> The stochastic nature of these contacts gives pause (not all OFF BCs of a given class make them), but they clearly function. The discovery of blue OFF midget BCs<sup>61</sup> might partly explain the sparse appearance of B-/Y+ neurons in the primate LGN<sup>197</sup> except for the fact that the fields of these cells tend to large and better match those of melanopsin GCs, whose dendrites likely never go near the terminals of blue OFF midget BCs. An exciting new concept in BC physiology is the idea that AMPA receptors and KA receptors are differentially expressed on dB3 and dB1/2 OFF cone BCs respectively, perhaps setting up the basis of fast (transient) and slow (sustained) BC channels<sup>64</sup> and matching GC contacts. If this is a basic format, then one might expect mGluR6-mediated transduction to vary in kinetics across classes of diffuse ON cone BCs. Specifically, might not dB4 resemble dB3 in being the 'fast' cone BC for the ON channel?

The ACs and the specialized, axon-bearing group we term association or AxCs (which include polyaxonal cells), remain our biggest challenge to understand. The diversity of AC dendritic arbors clearly does not fit a simplistic world of ACs monostratified for corresponding BCs<sup>44</sup> but does argue for highly circuit-selective functions.<sup>195</sup> It is possible that glycine AC systems are biased to signal across BC channels while GABA AC systems mostly signal within BC channels. The signaling of GABA receptors remains complex and likely finely tuned. Each conventional inhibitory synapse access a mixture of receptors or individually pure receptor patches. This fine-scale analysis is just beginning.

The cohort of GCs has been better circumscribed over the past decade, but has also become far more complex with the advent of multimodal melanopsin GC signaling and more cell classes than we have models for. We are closer than ever to understanding how DS GCs work, though study of such cells in primates is just beginning. Many classes of GCs clearly have more to do with the optical 'plant' of the eye; guiding fast and fine eye movements, driving foveation, discriminating self-movement from world-movement, creating the optic flow field, harmonizing visual drift and vestibular information, etc These essential functions, which are likely nonperceptual, likely involve more types of GCs than the major perceptual

pathways,<sup>1</sup> which in turn demand the bulk of retinal wiring. Further classification and reconstructing the connectivity of diverse GC classes remains a key target for the next decade.

In the end, why should such effort be applied to the details and the nuances of neuronal form and retinal circuitry? First, discoveries based on new molecular imaging tools continue to challenge any simplistic model of retinal organization by finding new cells, new contacts and new functions in the retina. Second, a range of inherited disorders arise from genes associated with building the neural retina and those genes represent both our evolutionary path and mechanisms we must understand if we are ever to make retinal repair a reality. Third, the details of wiring and global control, and the scope and speed of disease-triggered rewiring reveal that the effects of many forms of retinal degenerations once thought to be restricted to the outer retina actually propagate aggressively into the neural retina and likely the brain. Learning the rules and molecular mechanisms underlying postnatal plasticity is required to realize retinal restoration in diseases and traumas we cannot yet prevent. Finally, the neural retina remains unbowed. Though we believe we have disclosed its essences, it is proving to be a far richer organ than anticipated.

Retinal neuroanatomy is not a static field. The accelerating pace of discoveries augurs major revelations in retinal circuitry in the next decade, rather than mere refinements of current views. Since the last revision of this chapter, over 1500 papers have been published with reference to cones alone; over 1000 on retinal GCs alone; over 1000 on ACs and BCs combined. Over half of the references cited herein have been published since the year 2000. Many of the references are reviews and space limitations prevent a traditional historical treatment of the literature. It is no longer practical to cite the first instance of an idea or discovery (e.g., Ramón y Cajal or Tartuferi), much less its most lucid modern declamation or important related papers. It is hoped that readers will use this chapter as a point of departure in a greater scientific and medical adventure.

## ACKNOWLEDGMENTS

These last lines are the most difficult. On 30 May 2006 Ramon F Dacheux passed away: too soon, too young, beloved, admired. A decade ago, Ray and Elio Raviola performed the monumental task of crafting the modern view of retinal neuroanatomy for *Principles and Practice of Ophthalmology*. Beautifully written and illustrated, it strongly guided my revisions, and I have retained many figures, but few references. After all, Ray left us with a living field replete with new concepts and mechanisms in retinal processing that deserve our rapt attention. I believe that nothing would have pleased him more than replacing an earlier classic reference with one of his most vivid recent accomplishments: Dacheux RF, Chimento MF, Amthor FR. Synaptic input to the on-off directionally selective ganglion cell in the rabbit retina. *J Comp Neurol* 2003; 456:267–278.

ED: The acknowledgement here appears to deserve to be retained, perhaps in some briefer form. Please check.

## REFERENCES

1. Oyster C: The human eye. New York: Sinauer; 1999.
2. Bayer BE: Color imaging array. US; 1976.
3. Marc RE: Retinal neurotransmitters. In: Chalupa LM, Werner J, eds. *The visual neurosciences*. Cambridge: MIT Press; 2004:315–330.
4. Wässle H: Parallel processing in the mammalian retina. *Nat Rev Neurosci* 2004; 5:747–757.
5. Copenhagen D: Excitation in the retina: the flow, filtering and molecules of visual signaling in the glutamatergic pathways from photoreceptors to ganglion cells. In: Chalupa LM, Werner J, eds. *The visual neurosciences*. Cambridge: MIT Press; 2004:320–333.
6. Slaughter M: Inhibition in the retina. In: Chalupa LM, Werner J, eds. *The visual neurosciences*. Cambridge: MIT Press; 2004:355–368.
7. Kamermans M, Fahrenfort I: Ephaptic interactions within a chemical synapse: hemichannel-mediated ephaptic inhibition in the retina. *Curr Opin Neurobiol* 2004; 14:531–541.
8. Vaney D: Retinal Amacrine Cells. In: Chalupa LM, Werner J, eds. *The visual neurosciences*. Cambridge: MIT Press; 2004: 395–409.9. Feng G, Mellor RH, Bernstein M, et al: Imaging neuronal subsets in transgenic mice expressing multiple spectral variants of GFP. *Neuron* 2000; 28:41–51.
10. Morgan J, Huckfeldt R, Wong RO: Imaging techniques in retinal research. *Exp Eye Res* 2005; 80:297–306.
11. Marc RE, BW Jones, CB Watt, Strettoi E: Neural remodeling in retinal degeneration. *Prog Retin Eye Res* 2003; 22:607–655.
12. Marc RE, BW Jones, Watt CB: Retinal remodeling: circuitry revisions triggered by photoreceptor degeneration. In: Pinaud, et al, eds. *Plasticity in the visual system: from genes to circuits*. Springer; 2005: 33–54.
13. Illing ME, Rajan RS, Bence NF, Kopito RR: A rhodopsin mutant linked to autosomal dominant retinitis pigmentosa is prone to aggregate and interacts with the ubiquitin proteasome system. *J Biol Chem* 2002; 37, 34150–34160.

AU: Please supply first 3 editor names in place of et al. if number of editors >4; otherwise, supply all the editor names. Also supply initials of editors in all references.

AU: References 41, 55, and 119 are not cited. Please check.

AU: Please supply publisher name.

14. Carroll R: Vertebrate paleontology and evolution. New York: W. H. Freeman and company; 1988:698.
15. Famiglietti EV, Kolb H: A bistratified amacrine cell and synaptic circuitry in the inner plexiform layer of the retina. *Brain Res* 1975; 84:293–300.
16. Strettoi E, Dacheux RF, Raviola E: Synaptic connections of rod bipolar cells in the inner plexiform layer of the rabbit retina. *J Comp Neurol* 1990; 295:449–466.
17. Strettoi E, Raviola E, Dacheux RF: Synaptic connections of the narrowfield, bistratified rod amacrine cell (AlI) in the rabbit retina. *J Comp Neurol* 1992; 325:152–168.
18. Sterling P: How retinal circuits optimize the transfer of visual information. In: Chalupa LM, Werner J, eds. *The visual neurosciences*. Cambridge: MIT Press; 2004:234–259.
19. Ishida A, Stell W, Lightfoot D: Rod and cone inputs to bipolar cells in goldfish retina. *J Comp Neurol* 1980; 191:315–335.
20. Graham DR, Overbeek PA, Ash JD: Leukemia inhibitory factor blocks expression of Crx and Nrl transcription factors to inhibit photoreceptor differentiation. *Invest Ophthalmol Vis Sci* 2005; 46:2601–2610.
21. Bumsted O'Brien KM, Cheng H, Jiang Y, et al: Expression of photoreceptor-specific nuclear receptor NR2E3 in rod photoreceptors of fetal human retina. *Invest Ophthalmol Vis Sci* 2004; 45:2807–2812.
22. Cheng H, Khanna H, Oh ECT, et al: Photoreceptor-specific nuclear receptor NR2E3 functions as a transcriptional activator in rod photoreceptors. *Hum Mol Genet* 2004; 13:1563–1575.
23. Register EA, Yokoyama R, Yokoyama S: Multiple origins of the green-sensitive opsin genes in fish. *J Mol Evol* 1994; 39:268–273.
24. Bumsted K, Hendrickson A: Distribution and development of short-wavelength cones differ between Macaca monkey and human fovea. *J Comp Neurol* 1999; 403:502–516.
25. Ahnelt PK, Kolb H, Pflug R: Identification of a subtype of cone photoreceptor, likely to be blue sensitive, in the human retina. *J Comp Neurol* 1987; 255:18–34.
26. Kouyama N, Marshak DW: Bipolar cell specific for blue cones in the macaque retina. *J Neurosci* 1992; 12:1233–1252.
27. Nathans J: The evolution and physiology of human color vision: insights from molecular genetic studies of visual pigments. *Neuron* 1999; 24:299–312.
28. Wang Y, Smallwood PM, Cowan M, et al: Mutually exclusive expression of human red and green visual pigment-reporter transgenes occurs at high frequency in murine cone photoreceptors. *Proc Natl Acad Sci USA* 1999; 96:5251–5256.
29. Wässle H, Regus-Leidig H, Haverkamp S: Expression of the vesicular glutamate transporter vGluT2 in a subset of cones of the mouse retina. *J Comp Neurol* 2006; 496:544–555.
30. Dkhissi-Benyahya O, Rieux C, Hut RA, Cooper HM: Immunohistochemical evidence of a melanopsin cone in human retina. *Invest Ophthalmol Vis Sci* 2006; 47:1636–1641.
31. Marc RE: Interplexiform cell connectivity in the outer retina. In: Archer S, Djarmgoz MBA, Vallergera S, eds. *Neurobiology of the vertebrate outer retina*. London: Chapman and Hall; 1995:369–393.
32. Wehman AM, Staub W, Meyers JR, et al: Genetic dissection of the zebrafish retinal stem-cell compartment. *Dev Biol* 2005; 281:53–65.
33. Perron M, Harris WA: Retinal stem cells in vertebrates. *Bioessays* 2000; 22:685–688.
34. Hoffert JR, Baeyens DA, Fromm PO: The resistance of teleost ocular tissues to oxygen toxicity. *Invest Ophthalmol* 1973; 12:858–861.
35. Kalloniatis M, Marc RE, Murry R: Amino acid signatures in the primate retina. *J Neurosci* 1996; 16:6807–6829.
36. Morgan JL, Dhirga A, Vardi N, Wong RO: Axons and dendrites originate from neuroepithelial-like processes of retinal bipolar cells. *Nat Neurosci* 2006; 9:85–92.
37. Brecha N: Peptide and peptide receptor expression and function in the vertebrate retina. In: Chalupa LM, Werner J, eds. *The visual neurosciences*. Cambridge: MIT Press; 2004:334–354.
38. Migdale K, Herr S, Klug K, et al: Two ribbon synaptic units in rod photoreceptors of macaque, human, and cat. *J Comp Neurol* 2003; 455:100–112.
39. Sterling P, Matthews G: Structure and function of ribbon synapses. *Trends Neurosci* 2005; 28:20–29.
40. Wilson M. Retinal Synapses. In: Chalupa LM, Werner J, eds. *The visual neurosciences*. Cambridge: MIT Press; 2004:279–303.
41. Matthews G: Synaptic mechanisms of bipolar cell terminals. *Vision Res* 1999; 39:2469–2476.
42. Marc RE, Jones BW: Molecular phenotyping of retinal ganglion cells. *J Neurosci* 2002; 22:413–427.
43. Rockhill RL, Daly FJ, MacNeil MA, et al: The diversity of ganglion cells in a mammalian retina. *J Neurosci* 2002; 22:3831–3843.
44. MacNeil MA, Heussy JK, Dacheux RF, et al: The shapes and numbers of amacrine cells: matching of photofilled with Golgi-stained cells in the rabbit retina and comparison with other mammalian species. *J Comp Neurol* 1999; 413:305–326.
45. Nelson R., Kolb H: On and off pathways in the vertebrate retina and visual system (2004). In: Chalupa LM, Werner J, eds. *The visual neurosciences*. Cambridge: MIT Press; 2004:260–278.
46. Perkins GA, Ellisman MH, Fox DA: Three-dimensional analysis of mouse rod and cone mitochondrial cristae architecture: bioenergetic and functional implications. *Mol Vis* 2003; 9:60–732003.
47. Ripps H: Cell death in retinitis pigmentosa: gap junctions and the 'bystander' effect. *Exp Eye Res* 2002; 74:327–336.
48. Chun MH, Grunert U, Martin PR, Wässle H: The synaptic complex of cones in the fovea and in the periphery of the macaque monkey retina. *Vision Res* 1996; 36:3383–3395.
49. Raviola E, Gilula NB: Gap junctions between photoreceptor cells in the vertebrate retina. *Proc Natl Acad Sci USA* 1973; 70:1677.
50. Raviola E, Gilula NB: Intramembrane organization of specialized contacts in the outer plexiform layer of the retina. A freeze fracture study in monkeys and rabbits. *J Cell Biol* 1975; 65:192–222.
51. Guldénagel M, Ammermüller J, Feigenspan A, et al: Visual transmission deficits in mice with targeted disruption of the gap junction gene connexin36. *J Neurosci* 2001; 21:6036–6044.
52. Deans MR, Volgyi B, Goodenough DA, et al: Connexin36 is essential for transmission of rod-mediated visual signals in the mammalian retina. *Neuron* 2002; 36:703–712.
53. Li W, DeVries SH: Separate blue and green cone networks in the mammalian retina. *Nat Neurosci* 2004; 7:751–756.
54. Hornstein EP, Verweij J, Schnapf J: Electrical coupling between red and green in primate retina. *Nat Neuroscience* 2004; 7:745–750.
55. Nelson R, Famiglietti EV, Kolb H: Intracellular staining reveals different levels of stratification for on and off-center ganglion cells in cat retina. *J Neurophysiol* 1978; 41:472–483.
56. Missotten L: The ultrastructure of the human retina. Brussels: Editions Arscia Uitgaven; 1965.
57. Kolb H: Organization of the outer plexiform layer of the primate retina: electron microscopy of Golgi impregnated cells. *Phil Trans R Soc Lond B* 1970; 258:261–283.
58. Dowling JE, Boycott BB: Organization of the primate retina: electron microscopy. *Proc R Soc Lond B* 1966; 166:80–111.
59. Boycott BB, Hopkins M: Cone synapses of a flat diffuse cone bipolar cell in the primate retina. *J Neurocytol* 1993; 22:765–778.
60. Tsukamoto Y, Morigiwa K, Ueda M, Sterling P: Microcircuits for night vision in mouse retina. *J Neurosci* 2001; 21:8616–8623.
61. Klug K, Herr S, Tran Ngo I, et al: Macaque retina contains an s-cone off midgate pathway. *J Neurosci* 2003; 23:9881–9887.
62. Li W, DeVries SH: Bipolar cell pathways for color and luminance vision in a dichromatic mammalian retina. *Nat Neurosci* 2006; 9:669–675.
63. Haverkamp S, Grunert U, Wässle H: Localization of kainate receptors at the cone pedicles of the primate retina. *J Comp Neurol* 2001; 436:471–486.
64. DeVries SH: Bipolar cells use kainate and AMPA receptors to filter visual information into separate channels. *Neuron* 2000; 28:847–856.
65. DeVries SH, Li W, Saszik S: Parallel processing in two transmitter microenvironments at the cone photoreceptor synapse. *Neuron* 2006; 50:735–748.
66. Boycott B, Wässle H: Parallel processing in the mammalian retina: the proctor lecture. *Invest Ophthalmol Vis Sci* 1999; 40:1313–1327.
67. Famiglietti EV Jr: Class I and class II ganglion cells of rabbit retina: a structural basis for X and Y (brisk) cells. *J Comp Neurol* 2004; 478:323–346.
68. Kolb H, Nelson R, Mariani A: Amacrine cells, bipolar cells and ganglion cells of the cat retina: a Golgi study. *Vision Res* 1981; 21:1081–1114.
69. Dacey DM, Peterson BB, Robinson FR, Gamlin PD: Fireworks in the primate retina: in vitro photodynamics reveals diverse LGN-projecting ganglion cell types. *Neuron* 2003; 37:15–27.
70. Yamada ES, Bordt AS, Marshak DW: Wide-field ganglion cells in macaque retinas. *Vis Neurosci* 2005; 22:383–393.

## RETINA AND VITREOUS

71. Coombs J, van der List D, Wang GY, Chalupa LM: Morphological properties of mouse retinal ganglion cells. *Neuroscience* 2006; 140:123-136.
72. Kolb H, Marshak DW: The midget pathways of the primate retina. *Doc Ophthalmol* 2003; 106:67-81.
73. Diller L, Packer OS, Verweij J, et al: L and M cone contributions to the midget and parasol ganglion cell receptive fields of macaque monkey retina. *J Neurosci* 2004; 24:1079-1088.
74. Dowling JE, Boycott BB: Organization of the primate retina: electron microscopy. *Proc R Soc Lond B* 1966; 166:80-111.
75. West RW, Dowling JE: Synapses onto different morphological types of retinal ganglion cells. *Science* 1972; 178:510-512.
76. Wässle H, Boycott BB, Illing RB: Morphology and mosaic of on and off beta cells in the cat retina and some functional considerations. *Proc R Soc Lond [B]* 1981; 212:177.
77. Jusuf PR, Martin PR, Grunert U: Random wiring in the midget pathway of primate retina. *J Neurosci* 2006; 26:3908-3917.
78. Jacoby RA, Marshak DW: Synaptic connections of db3 diffuse bipolar cell axons in macaque retina. *J Comp Neurol* 2000; 416:19-29.
79. Calloway EM: Cell types and local circuits in primary visual cortex of the macaque monkey. In Chalupa LM, Werner J, eds. *The visual neurosciences*. Cambridge: MIT Press; 2004:680-694.
80. Masland RH: Directional selectivity in retinal ganglion cells. In Chalupa LM, Werner J, eds. *The visual neurosciences*. Cambridge: MIT Press; 2004:451-562.
81. Yamada ES, Dmitrieva N, Keyser KT, et al: Synaptic connections of starburst amacrine cells and localization of acetylcholine receptors in primate retinas. *J Comp Neurol* 2003; 461:76-90.
82. Dacey DM, Lee BB: The blue-ON opponent pathway in primate retina originates from a distinct bistratified ganglion cell type. *Nature* 1994; 367:731-735.
83. Dacey DM, Liao HW, Peterson BB, et al: Melanopsin-expressing ganglion cells in primate retina signal colour and irradiance and project to the LGN. *Nature* 2005; 433:749-754.
84. Berson DM, Dunn FA, Takao M: Phototransduction by retinal ganglion cells that set the circadian clock. *Science* 2002; 295:1070-1073.
85. Hattar S, Lucas RJ, Mrosovsky N, et al: Melanopsin and rod-cone photoreceptive systems account for all major accessory visual functions in mice. *Nature* 2003; 424:76-81.
86. Tu DC, Zhang D, Demas J, et al: Physiologic diversity and development of intrinsically photosensitive retinal ganglion cells. *Neuron* 2005; 48:987-999.
87. Lucas RJ, Hattar S, Takao M, et al: Diminished pupillary light reflex at high irradiances in melanopsin-knockout mice. *Science* 2003; 299:245-247.
88. Fu Y, Zhong H, Wang MH, et al: Intrinsically photosensitive retinal ganglion cells detect light with a vitamin A-based photopigment, melanopsin. *Proc Natl Acad Sci USA* 2005; 102:10339-10344.
89. Freedman MS, Lucas RJ, Soni B, et al: Regulation of mammalian circadian behavior by non-rod, non-cone, ocular photoreceptors. *Science* 1999; 284:502-504.
90. Silva MM, Albuquerque AM, Araujo JF: Light-dark cycle synchronization of circadian rhythm in blind primates. *J Circadian Rhythms* 2005; 3:10.
91. Marc RE: 1999 Mapping glutamatergic drive in the vertebrate retina with a channel permeant organic cation. *J Comp Neurol* 1999; 407:47-64.
92. Marc RE: Kainate activation of horizontal, bipolar, amacrine and ganglion cells in the rabbit retina. *J Comp Neurol* 1999; 407:65-76.
93. Vaney DI, Weiler R: Gap junctions in the eye: evidence for heteromeric, heterotypic and mixed-homotypic interactions. *Brain Res Brain Res Rev* 2000; 32:115-120.
94. Kenyon GT, Marshak DW: Gap junctions with amacrine cells provide a feedback pathway for ganglion cells within the retina. *Proc Biol Sci* 1998; 265:919-925.
95. Marc RE: The structure of GABAergic circuits in ectotherm retinas. In: Mize R, Marc RE, Sillito A, eds. *GABA in the retina and central visual system*. Elsevier: Amsterdam; 1992:61-92.
96. Dacheux RF, Raviola E: Horizontal cells in the retina of the rabbit. *J Neurosci* 1982; 2:1486-1493.
97. Raviola E, Dacheux RF: Variations in structure and response properties of horizontal cells in the retina of the rabbit. *Vision Res* 1983; 23:1221-1227.
98. Nelson R: Cat cones have rod input: a comparison of the response properties of cones and horizontal cell bodies in the retina of the cat. *J Comp Neurol* 1977; 172:109-136.
99. Fisher SK, Boycott BB: Synaptic connexions made by horizontal cells within the outer plexiform layer of the retina of the cat and rabbit. *Proc R Soc Lond B* 1974; 186:317-331.
100. Peichl L, González-Soriano J: Morphological types of horizontal cell in rodent retinas: a comparison of rat, mouse, gerbil, and guinea pig. *Vis Neurosci* 1994; 11:501-517.
101. Perlman I, Kolb H, Nelson R: Anatomy, circuitry, and physiology of vertebrate horizontal cells. In Chalupa LM, Werner J, eds. *The visual neurosciences*. Cambridge: MIT Press; 2004:369-394.
102. Boycott BB, Kolb H: The horizontal cells of the rhesus monkey retina. *J Comp Neurol* 1973; 148:115-140.
103. Kolb H, Mariani A, Gallego A: A second type of horizontal cell in the monkey retina. *J Comp Neurol* 1980; 189:31-44.
104. Kolb H, Fernandez E, Schouten J, et al: Are there three types of horizontal cell in the human retina? *J Comp Neurol* 1994; 343:370-386.
105. Wässle H, Dacey DM, Haun T, et al: The mosaic of horizontal cells in the macaque monkey retina: with a comment on biplexiform ganglion cells. *Vis Neurosci* 2000; 17:591-608.
106. Dacheux RF, Raviola E: Physiology of HI horizontal cells in the primate retina. *Proc R Soc Lond B* 1990; 239:213-230.
107. Dacey DM, Lee BB, Stafford DK, et al: Horizontal cells of the primate retina: cone specificity without spectral opponency. *Science* 1996; 271:656-659.
108. Dacey DM: Parallel pathways for spectral coding in primate retina. *Annu Rev Neurosci* 2000; 23:743-775.
109. Blanco R, de la Villa P: Ionotropic glutamate receptors in isolated horizontal cells of the rabbit retina. *Eur J Neurosci* 1999; 11:867-873.
110. Haverkamp S, Grunert U, Wässle H: The synaptic architecture of AMPA receptors at the cone pedicle of the primate retina. *Neurosci* 2001; 21:2488-2500.
111. Lindberg KA, Fisher SK: Ultrastructural evidence that horizontal cell axon terminals are presynaptic in the human retina. *J Comp Neurol* 1988; 268:281-297.
112. Setou M, Seog D-H, Tanaka Y, et al: Glutamate-receptor-interacting protein GRIP1 directly steers kinesin to dendrites. *Nature* 2002; 417:83-87.
113. Kamermans M, Fahrenfort I, Schultz K, et al: Hemichannel-mediated inhibition in the outer retina. *Science* 2001; 292:1178-1180.
114. Mills SL, Massey SC: Distribution and coverage of A- and B-type horizontal cells stained with Neurobiotin in the rabbit retina. *Vis Neurosci* 1994; 11:549-560.
115. Mills SL, Massey SC: A series of biotinylated tracers distinguishes three types of gap junction in retina. *J Neurosci* 2000; 20:8629-8636.
116. Packer OS, Dacey DM: Synergistic center-surround receptive field model of monkey H1 horizontal cells. *J Vision* 2005; 5:1038-1054.
117. Wagner HJ, Wagner E: Amacrine cells in the retina of a teleost fish, the road (Rutilus rutilus): a Golgi study on differentiation and layering. *Phil Trans Roy Soc Lond B* 321: 263-324.
118. Pourcho RG, Goebel DJ: A combined Golgi and autoradiographic study of (<sup>3</sup>H) glycine accumulating amacrine cells in the cat retina. *J Comp Neurol* 1985; 233:473-480.
119. Vaney DI: The morphology and topographic distribution of all amacrine cells in the cat retina. *Proc Roy Soc (Lond)* 1985; 224:475-488.
120. Tauchi M, Masland RH: The shape and arrangement of the cholinergic neurons in the rabbit retina. *Proc R Soc Lond B* 1984; 223:101-119.
121. Famiglietti EV Jr: Synaptic organization of starburst amacrine cells in rabbit retina: analysis of serial thin sections by electron microscopy and graphic reconstruction. *J Comp Neurol* 1991; 309:40-70.
122. Sandell JH, Masland RH: A system of indoleamine-accumulating neurons in the rabbit retina. *J Neurosci* 1986; 6:3331-3347.
123. Vaney DI: Morphological identification of serotonin-accumulating neurons in the living retina. *Science* 1986; 233:444-446.
124. Sandell JH, Masland RH, Raviola E, Dacheux RF: Connections of indoleamine-accumulating cells in the rabbit retina. *J Comp Neurol* 1989; 283:303-313.
125. Li W, Zhang J, Massey SC: Coupling pattern of S1 and S2 amacrine cells in the rabbit retina. *Vis Neurosci* 2002; 19:119-131.
126. Rodieck RW, Marshak DW: Spatial density and distribution of choline acetyltransferase immunoreactive cells in human, macaque, and baboon retinas. *J Comp Neurol* 1992; 321:46-64.
127. Springer AD, Hendrickson AE: Development of the primate area of high acuity, 3: temporal relationships between pit formation, retinal elongation and cone packing. *Vis Neurosci* 2005; 22:171-185.
128. Hendrickson A, Troilo D, Possin D,

AU: Please supply last page number for all journal type references, if available.

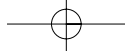
AU: Please supply the correct year.

AU: Please supply year of publication.



- Springer A: Development of the neural retina and its vasculature in the marmoset *Callithrix jacchus*. *J Comp Neurol* 2006; 497:270–286.
129. Curcio CA, Sloan KR, Kalina RE, Hendrickson AE: Human photoreceptor topography. *J Comp Neurol* 1990; 292:497–523.
130. Jeon CJ, Strettoi E, Masland RH: The major cell populations of the mouse retina. *J Neurosci* 1998; 18:8936–8946.
131. Remtulla S, Hallett PE: A schematic eye for the mouse, and comparisons with the rat. *Vis Res* 1985; 25:21–31.
132. Szel IA, Rohlich P, Caffé AR, et al: Unique topographic separation of two spectral classes of cones in the retina. *J Comp Neurol* 1992; 325:327–342.
133. Juliusson B, Bergstrom A, Rohlich P, et al: Complementary cone fields of the rabbit retina. *Invest Ophthalmol Vis Sci* 1994; 35:811–818.
134. Lukats A, Szabo A, Rohlich P, et al: Photopigment coexpression in mammals: comparative and developmental aspects. *Histol Histopathol* 2005; 20:551–574.
135. Marc RE, Sperling HG: The chromatic organization of primate cones. *Science* 1977; 196:454–456.
136. Curcio CA, Allen KA, Sloan KR, et al: Distribution and morphology of human cone photoreceptors stained with anti-blue opsin. *J Comp Neurol* 1991; 312:610–624.
137. Cornish EE, Madigan MC, Natoli R, et al: Gradients of cone differentiation and FGF expression during development of the foveal depression in macaque retina. *Vis Neurosci* 2005; 22:447–459.
138. Grünbaum B, Shephard GC: Tilings and patterns. New York: WH Freeman; 1987:700.
139. Cook JE. Spatial regularity among retinal neurons. In Chalupa LM, Werner J, eds. *The visual neurosciences*. Cambridge: MIT Press; 2004:463–478.
140. Cook JE: Spatial properties of retinal mosaics: an empirical evaluation of some existing measures. *Vis Neurosci* 1996; 13:15–30.
141. Engstrom K, Ahlbert IB: Cone types and cone arrangement in the retina of some flatfishes. *Acta Zool* 1963; 44:1–11.
142. Kalloniatis M, RE Marc: Interplexiform cells of the goldfish retina. *J Comp Neurol* 1990; 297:340–358.
143. Reese BE, Galli-Resta L: The role of tangential dispersion in retinal mosaic formation. *Prog Ret Eye Res* 2002; 21:153–168.
144. Wong ROL, Godhino L: Development of the vertebrate retina. In Chalupa LM, Werner J, eds. *The visual neurosciences*. Cambridge: MIT Press; 2004:77–94.
145. Mariani AP: Biplexiform cells: ganglion cells of the primate retina that contact photoreceptors. *Science* 1982; 216:1134–1136.
146. Trexler EB, Li W, Massey SC: Simultaneous contribution of two rod pathways to All amacrine and cone bipolar cell light responses. *J Neurophysiol* 2005; 93:1476–1485.
147. Saszik SM, Robson JG, Frishman LJ: The scotopic threshold response of the dark-adapted electrophoretogram of the mouse. *J Physiol* 2002; 543:899–916.
148. Li W, Keung JW, Massey SC: Direct synaptic connections between rods and OFF cone bipolar cells in the rabbit retina. *J Comp Neurol* 2004; 474:1–12.
149. Reid RC, Shapley RM: Spatial structure of cone inputs to receptive fields in primate lateral geniculate nucleus. *Nature* 1992; 356:716–718.
150. Lee BB, Kremers J, Yeh T: Receptive fields of primate retinal ganglion cells studied with a novel technique. *Vis Neurosci* 1998; 15:161–175.
151. Sun H, Smithson HE, Zaidi Q, Lee BB: Specificity of cone inputs to macaque retinal ganglion cells. *J Neurophys* 2006; 95:837–849.
152. Calkins DJ, Sterling P: Absence of spectrally specific lateral inputs to midget ganglion cells in primate retina. *Nature* 1996; 381:613–615.
153. Dacey D, Packer OS, Diller L, et al: Center surround receptive field structure of cone bipolar cells in primate retina. *Vision Res* 2000; 40:1801–1811.
154. Williams DR, Hofer H. Formation and Acquisition of the Retinal Image. In Chalupa LM, Werner J, eds. *The visual neurosciences*. Cambridge: MIT Press; 2004.
155. Roorda A, Williams DR: The arrangement of the three cone classes in the living human eye. *Nature* 1999; 397:520–522.
156. Hofer H, Carroll J, Neitz J, et al: Organization of the human trichromatic cone mosaic. *J Neurosci* 2005; 25:9669–9679.
157. Kolb H, Dekorver L: Midget ganglion cells of the parafovea of the human retina: a study by electron microscopy and serial section reconstructions. *J Comp Neurol* 1991; 303:617–636.
158. Brainard DH, Roorda A, Yamauchi Y, et al: Functional consequences of the relative numbers of L and M cones. *J Opt Soc Am A* 2000; 17:607–614.
159. Xiao Y, Wang Y, Felleman DJ: A spatially organized representation of colour in macaque cortical area V2. *Nature* 2003; 421:535–539.
160. Neitz J, Carroll J, Yamauchi Y, et al: Color perception is mediated by a plastic neural mechanism that is adjustable in adults. *Neuron* 2002; 35:783–792.
161. Marc RE, Liu WL: Fundamental GABAergic amacrine cell circuitries in the retina: nested feedback, concatenated inhibition, and axosomatic synapses. *J Comp Neurol* 2000; 425:560–582.
162. Dubin MW: The inner plexiform layer of the vertebrate retina: a quantitative and comparative electron microscopic analysis. *J Comp Neurol* 1970; 140:479–505.
163. Hennig MH, Funke K, Wörgötter F: The influence of different retinal subcircuits on the nonlinearity of ganglion cell behavior. *J Neurosci* 2002; 22:8726–8738.
164. Dacheux RF, Chimento MF, Amthor FR: Synaptic input to the on-off directionally selective ganglion cell in the rabbit retina. *J Comp Neurol* 2003; 456:267–278.
165. Cajal SR: *La rétine des vertébrés*. La Cellule 1893; 9:119–257.
166. Polyak SL: *The retina*. Chicago: University of Chicago Press; 1941.
167. Gastinger MJ, O'Brien JJ, Larsen NB, Marshak DW: Histamine immunoreactive axons in the macaque retina. *Invest Ophthalmol Vis Sci* 1999; 40:487–495.
168. Gastinger MJ, Barber AJ, Khin SA, et al: Abnormal centrifugal axons in streptozotocin-diabetic rat retinas. *Invest Ophthalmol Vis Sci* 2001; 42:2679–2685.
169. Gastinger MJ, Bordt AS, Bernal MP, Marshak DW: Serotonergic retinopetal axons in the monkey retina. *Curr Eye Res* 2005; 30:1089–1095.
170. Gastinger MJ, Barber AJ, Vardi N, Marshak DW: Histamine receptors in mammalian retinas. *J Comp Neurol* 2006; 495:658–667.
171. Witkovsky P: Dopamine and retinal function. *Doc Ophthalmol* 2004; 108:17–39.
172. Dacey DM: The dopaminergic amacrine cell. *J Comp Neurol* 1990; 301:461–489.
173. Nguyen-Legros J: Morphology and distribution of catecholamine neurons in mammalian retina. In: Osborne NN, Chader G, eds. *Progress in retinal research*. Oxford: Pergamon; 1988:113–147.
174. Mariani AP, Hokoc JN: Two types of tyrosine hydroxylase-immunoreactive amacrine cell in the rhesus monkey retina. *J Comp Neurol* 1988; 276:81–91.
175. Oh SJ, Kim IB, Lee EJ, et al: Immunocytochemical localization of dopamine in the guinea pig retina. *Cell Tissue Res* 1999; 298:561–565.
176. Zhang D-Q, Stone JF, Zhou T, et al: Characterization of genetically labeled catecholamine neurons in the mouse retina. *Neuroreport* 2004; 15:1761–1765.
177. Feigenspan A, Gustincich S, Bean BP, Raviola E: Spontaneous activity of solitary dopaminergic cells of the retina. *J Neurosci* 1998; 18:6776–6789.
178. Xiao J, Cai Y, Yen J, et al: Voltage-clamp analysis and computational model of dopaminergic neurons from mouse retina. *Vis Neurosci* 2004; 21:835–849.
179. Hampson EC, Vaney DI, Weiler R: Dopaminergic modulation of gap junction permeability between amacrine cells in mammalian retina. *J Neurosci* 1992; 12:4911–4922.
180. Ishida AT: In: Chalupa LM, Werner J, eds. *The visual neurosciences*. Cambridge: MIT Press; 2004:422–450.
181. Ruan GX, Zhang DQ, Zhou T, et al: Circadian organization of the mammalian retina. *Proc Natl Acad Sci USA*. 2006; epub ahead of print.
182. Wiechmann AF: Regulation of gene expression by melatonin: a microarray survey of the rat retina. *J Pineal Res* 2002; 33:178–185.
183. Eldred WD, Blute TA: Imaging of nitric oxide in the retina. *Vision Res* 2005; 45:3469–3486.
184. Mills SL, Massey SC: Differential properties of two gap junctional pathways made by All amacrine cells. *Nature* 1995; 377:734–737.
185. Kao YH, Lassova L, Bar-Yehuda T, et al: Evidence that certain retinal bipolar cells use both glutamate and GABA. *J Comp Neurol* 2004; 478:207–218.
186. Newman EA: Glial modulation of synaptic transmission in the retina. *Glia* 2004; 47:268–274.
187. Kawamura H, Sugiyama T, Wu DM, et al: ATP: a vasoactive signal in the pericyte-containing microvasculature of the rat retina. *J Physiol* 2005; 551:787–799.
188. Zalutsky RA, Miller RF: The physiology of somatostatin in the rabbit retina. *J Neurosci* 1990; 10:383–393.
189. Johnson J, Caravelli ML, Brecha NC: Somatostatin inhibits calcium influx into rat rod bipolar cell axonal terminals. *Vis*

AU: Please supply chapter title.  
AU: Please supply volume number and page range.



## RETINA AND VITREOUS

---

- Neurosci 2001; 18:101–108.
190. Tian N, Copenhagen DR: Visual deprivation alters development of synaptic function in inner retina after eye opening. *Neuron* 2001; 32:439–449.
191. Tian N: Visual experience and maturation of retinal synaptic pathways. *Vision Res* 2004; 44:3307–3316.
192. Fisher SK, Lewis GP, Linberg KA, Verardo MR: Cellular remodeling in mammalian retina: results from studies of experimental retinal detachment. *Prog Retin Eye Res* 2005; 24:395–431.
193. Jones BW, Marc RE: Retinal remodeling during retinal degeneration. *Exp Eye Res* 2005; 81:121–244.
194. Marc RE, Jones BW, Watt CB: Retinal remodeling: circuitry revisions triggered by photoreceptor degeneration. In: Pinaud, et al, eds. *Plasticity in the visual system: from genes to circuits*. Springer; 2005; 33–54.
195. Masland RH: The fundamental plan of the retina. *Nat Neurosci* 2004; 4:877–886.
196. Ochs M, Mayhew TM, Knabe W: To what extent are the retinal capillaries ensheathed by muller cells? A stereological study in the tree shrew *Tupaia belangeri*. *J Anat* 2000; 196:453–461.
197. Chatterjee S, Callaway EM: Parallel colour-opponent pathways to primary visual cortex. *Nature* 2003; 426:668–671.

